Step-wise Adjustable Iterated Function Systems

By

TYNAN CODY LAZARUS

DISSERTATION

Submitted in partial satisfaction of the requirements for the degree of

DOCTOR OF PHILOSOPHY

in

MATHEMATICS

in the

OFFICE OF GRADUATE STUDIES

of the

UNIVERSITY OF CALIFORNIA

DAVIS

Approved:

Qinglan Xia

John Hunter

Janko Gravner

Committee in Charge

2019

To my parents for their unwavering belief in their children.

Contents

Abstract iv

Acknowledgments v

Chapter 1. Introduction 1

1.1. History 1

1.2. Measures and Dimensions 7

1.3. Other Notions of Dimension 16

Chapter 2. Moran Sets and Iterated Function Systems 24

2.1. Moran Sets 24

2.2. Iterated Function Systems 27

Chapter 3. $\mathcal{F}-$Limit Sets 35

3.1. Hausdorff Dimension of the Limit Sets 36

3.2. General Setup of $\mathcal{F}$-Limit sets 40

3.3. Hausdorff dimensions of $\mathcal{F}$-Limit sets 42

3.4. Examples of $\mathcal{F}$-Limit sets 47

3.5. Uniform Covering Condition 63

Appendix A. Matlab Code for Figures 72

A.1. Cantor Set functions 72

A.2. Sierpinski Triangle functions 74

A.3. Menger Sponge functions 80

Bibliography 86

Step-wise Adjustable Iterated Function Systems

Abstract

Fractals have caught the attention of the public over the last few decades with their often beautiful colors or naturalistic look. However, the math underlying the beautiful images has not become as mainstream, even though the classical ways to generate fractals using Moran sets or Iterated Function Systems (IFS) is relatively straightforward. In this thesis we start with some common examples and ways to generate fractals, as well as the common measures and dimensions used to analyze fractals. We then present a new process that mixes the Moran set and IFS generating techniques by allowing the generating process to be updated at each iteration, which produces non-self-similar fractals with more variation but does not change the computational complexity when compared to a standard IFS construction. We then provide estimates and calculations for the Hausdorff dimension of the new fractals generated from this process.

Acknowledgments

Making it to the end of this journey of grad school would not have been possible without the support of those around me. I would like to first thank my adviser Qinglan Xia for his patience, kindness, and support in all aspects of my time in Davis. There was never a question that I felt too embarrassed to ask, and the conversations and insights into teaching have been helpful beyond recognition. In a world where most professors want their students to only follow in the same path as themselves, I lucked out and found an adviser that cared for my interests and goals and did not try to change them. I would also like to thank Tina Denena, Sarah Driver, Matthew Silver, and the other staff in the math office that have dealt with my constant interruptions and questions over the last half of a decade. Your moral support in my darker times and your exuberance in my triumphs have not gone unnoticed. I will forever be grateful for your encouragement and support through each part of my degree. I would like to thank the lecturers in the department for allowing me to incessantly pester them with questions, and for helping me to find and formulate my teaching style. Your enthusiasm for teaching has helped to fan mine, and the educational value of the department would be much less without you. Lastly, I would like to thank my friends and family for the long hours of supportive phone calls, distractions, love and commitment. Without that love as my backbone, I would not have made it all the way through to finishing.

CHAPTER 1

Introduction

1.1. History

Although fractal geometry blossomed in the 1970's and 80's, it has roots as far back as the nineteenth century. Without the tools to fully understand a fractal, the curves that seemed to have rather odd properties were called "monsters". One of the first to rigorously describe such a monster curve was Weierstrass in 1872 with the function

$$f(x) = \sum_{n=1}^{\infty} b^n \cos(a^n x\pi), \tag{1.1.1}$$

where $b \in (0,1)$ and $a \in \mathbb{Z}_{\geq 0}$.

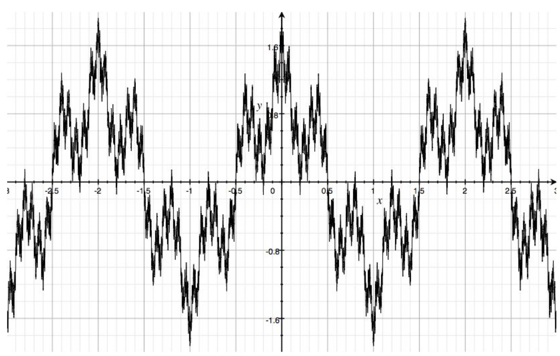

FIGURE 1.1. Weierstrass function with $b = 0.5, a = 5$, 500 terms

Weierstrass showed that this function is continuous but nowhere differentiable. Although there was no way to graph the function to see what this behavior may look like, this was the first proven example with such properties. At the time, most of mathematics was concerned with differentiable and smooth curves.

In 1883 Georg Cantor defined another function with odd properties (the function, $F_{\mathcal{C}}(x)$, later became known as the Cantor function or the Devil's staircase). One can see from Figure 1.2 that this function $F_{\mathcal{C}}(x)$ is non-constant, monotonic, continuous, and has $F'_{\mathcal{C}}(x) = 0$ almost everywhere.

The set of points where $F'_{\mathcal{C}}(x)$ is not defined is the set that now bears Cantor's name (later we will formally define the Cantor set $\mathcal{C}$). The Cantor set has become arguably one of the most important sets in set theory, and was a key example for Felix Hausdorff to base his revolutionary paper [**16**] on.

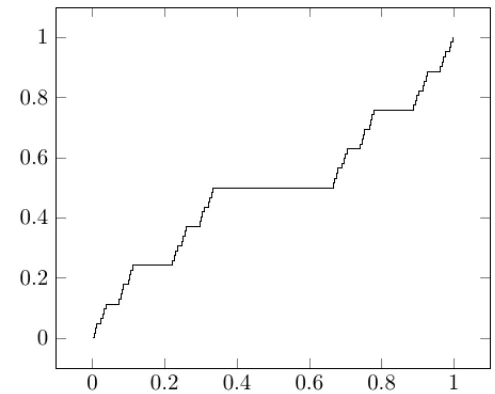

FIGURE 1.2. The Cantor function $F_{\mathcal{C}}(x)$

Helge von Koch was dissatisfied with Weierstrass' function because of the lack of ability to see it, so in 1904 he made a construction of a curve that would have similar properties (continuous but no-where differentiable) from a purely geometric construction. The curve is now commonly known as Koch's curve, or the Koch snowflake when three of the curves are put together in a triangular formation. This curve has become another of the classic examples of a fractal, even though it was created more than half a century before the term was coined. Even so, there wasn't much framework to study these objects, as they were mainly developed as pathological counterexamples to established theory for smooth curves.

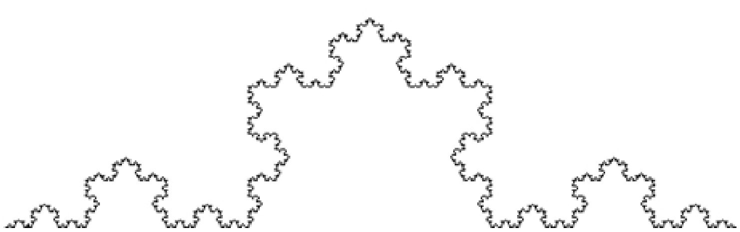

(A) The Koch curve

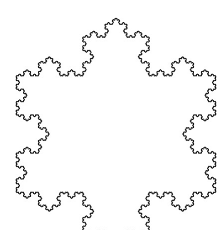

(B) The Koch Snowflake

That changed in 1918 when Hausdorff published [**16**], a paper describing a new set of measures that generalized Lebesgue measure to non-integral dimensions. This new definition of dimension has become one of the central ways to study fractal sets and will be discussed more fully in chapter 2.

At the same time Gaston Julia and Pierre Fatou were developing the theory of iterative functions in the complex plane. In particular, the basins of attraction that were defined by Julia tended to have fractal boundaries. This line of research would also become important in chaos theory, which has numerous connections with fractal geometry. Only when computers where invented did the connections to fractal geometry become apparent, however. For a more complete treatment of this, see [**15**].

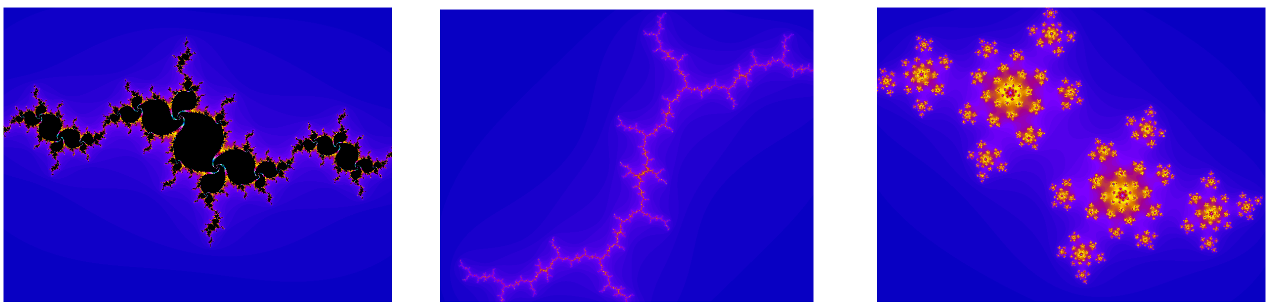

(A) connected (B) dendrite (C) disconnected

FIGURE 1.4. Types of Julia sets

This area would remain rather stagnant until the invention of computers, and their power of visualization in the hands of Benoit Mandelbrot. Mandelbrot coined the term "fractal", and gave a name to this area of mathematics. In his seminal paper [**25**] of 1983, Mandelbrot was especially interested in the ability of these nondifferentiable structures to model natural objects and settings since nature doesn't seem to use perfectly smooth objects. Mandelbrot used examples of clouds, rivers, mountains, and coastlines as objects that do not fit in with Euclidean geometry. He also was able to show the connection between Hausdorff's measures and the sets that were constructed by Fatou and Julia. The famous Mandelbrot set (illustrate in Figure 1.5) is named after him since he was the first to produce an image of the set and describe some of its properties. In doing so, he set forth the groundwork for much work to be done in visualizing and understanding these monster curves and sets in a whole new way.

The fact that these rough fractal objects were usually created and described from smooth dynamical systems made them easier to adapt to various real-world systems. Fractals have been

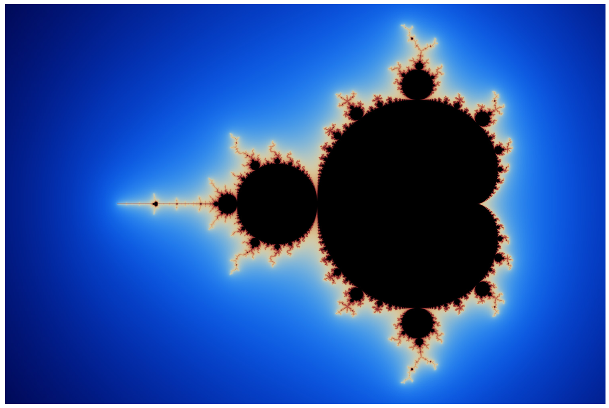

FIGURE 1.5. The Mandelbrot set

used in physics to model rough terrain, in image compression and computer graphics, in stockmarket analysis, in ecology to measure the health and growth of forests... We have only begun to scratch the surface of applications, especially with analysis of big data and social networks taking the mathematical community by storm.

We have yet to discuss a definition of a fractal, and for good reason. Across the literature, there isn't an agreed upon, rigorous definition that is used! Mandelbrot gave an initial definition, expressed in (1.2.6), but even he did not keep it for long. In general, we will consider a set F to be a fractal if it satisfies most of the following properties:

- F has some form of self-similarity at all scales, even statistical in nature
- F contains detailed structure at arbitrarily small scales
- F and its local structure cannot be described readily with classical analytical tools
- The construction of F is straightforward (often recursive)

First, let's construct some examples to have in mind. We start with a fractal made from intervals.

EXAMPLE 1.1.1 (Cantor Set). We begin with the unit interval $E_0 = [0, 1]$. For the first generation, we divide E_0 into three equal subintervals, each $1/3$ the length and remove the open middle third set. So $E_1 = [0, 1/3] \cup [2/3, 1]$. To create the second generation, we apply the same process to each interval in E_1. Thus, $E_2 = [0, 1/9] \cup [2/9, 1/3] \cup [2/3, 7/9] \cup [8/9, 1]$. Continuing this process forever, we get a sequence of nested sets $\{E_n\}_{n=0}^{\infty}$. The Cantor set is defined to be

$$\mathcal{C} := \bigcap_n E_n. \tag{1.1.2}$$

An alternative way to define the Cantor set is by using a base-3 expansion of the numbers in $[0,1]$. Since the construction of $\mathcal{C}$ does not included points from the middle set at each stage, we only include the points in $[0,1]$ with no $1'$s in their base-3 expansion. That is,

$$\mathcal{C} = \{x = 0.a_1a_2a_3\cdots \mid a_n \in \{0,2\} \text{ for all } n \in \mathbb{N}. \tag{1.1.3}$$

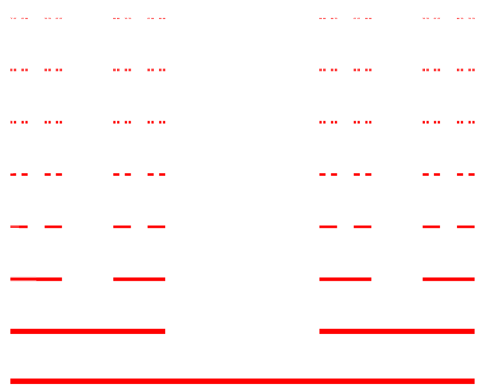

FIGURE 1.6. Construction of the Cantor set

Next we describe the construction of a fractal from triangles.

EXAMPLE 1.1.2 (Sierpinski Triangle). Define E_0 to be an equilateral triangle with unit side length. To create the first generation E_1, we connect the midpoints of each side, creating four triangles of side length $1/2$. We remove the inverted open middle triangle that does not share a vertex with E_0. For E_2, we apply the same rule to the three remaining triangles and take the union of the remaining pieces (see Figure 1.7). As with the Cantor set, we continue this process indefinitely to obtain a sequence of nested sets $\{E_n\}_{n=0}^{\infty}$, and define the Sierpinski Triangle (or Sierpinski Gasket) to be the set

$$F = \bigcap_n E_n. \tag{1.1.4}$$

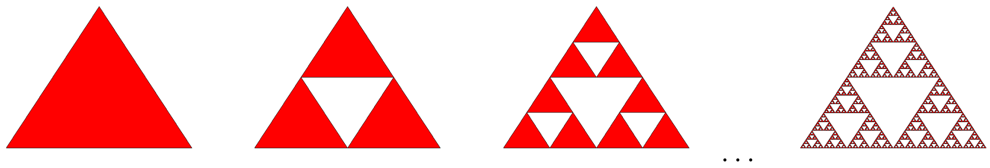

FIGURE 1.7. Constructing the Sierpinski triangle

EXAMPLE 1.1.3 (Menger Sponge). Let E_0 be the unit cube. Next, we cut the cube into 27 smaller cubes, each with side length 1/3. To create E_1, we remove the open middle cube from each face, as well as the open smaller cube at the center of E_0. Thus, we are left with 20 cubes of length 1/3 that comprise E_1. Continuing in this process of removing the middle cube from each face and the center, we obtain a sequence of nested sets $\{E_n\}_{n=0}^{\infty}$. We define the Menger sponge to be the limiting set,

$$F = \bigcap_n E_n. \tag{1.1.5}$$

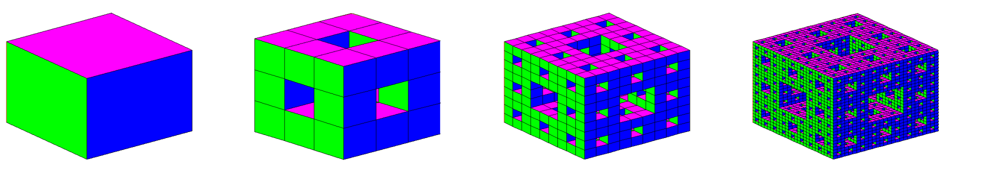

FIGURE 1.8. Constructing the Menger cube

EXAMPLE 1.1.4. The Koch curve is constructed from line segments. We start with E_0 being the line segment $[0, 1]$. To create E_1, we divide E_0 into three equal subintervals and replace the middle interval by the other two sides of an equalateral triangle. Thus, E_1 contains four line segments that are all 1/3 the length of the original E_0. Then E_2 is created by applying the same rule to each of the four line segments in E_1. Continuing this process ad infinitum, the Koch curve will be the resulting limit set. See Figure 1.9.

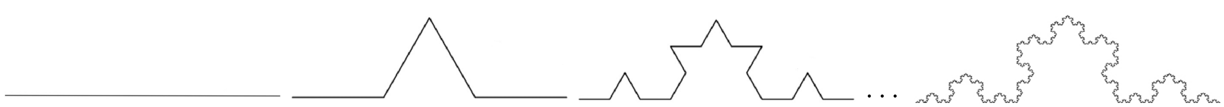

FIGURE 1.9. Constructing the Koch Curve

We can see that in the construction of each of these examples, each property is satisfied:

- Each fractal is exactly self-similar because each new generation is a specific number of copies of the previous generation.
- Each generation increases the number of pieces exponentially, and since they are similar to the original, one can see the same patterns at all scales.
- The fractals are rather hard to describe without speaking of it as a limit of a process. The Cantor set is made of an intersection of intervals, but is a collection of points. In fact, it is an uncountable collection of points that has length 0 (for proof, see [**12**]).
- Each construction just takes an initial object and a rule of how to create a new generation, and iteratively applies the rule to each new generation.

However, with these properties as the definition, we may include sets that most people wouldn't consider to be fractal. For example, notice that the set of rational number $\mathbb{Q}$ satisfies all the properties. But in terms of being a fractal, it doesn't have the same sort of striking shape that these other examples have. In fact, according to Mandelbrot's original definition, the rational numbers would not be considered a fractal. As we will see in a future example, even such a simple set as a sequence of real numbers together with its limit could be considered fractal when measuring it from specific points of view. Thus, we will leave the definition fluid and use the bullet points as a guideline.

1.2. Measures and Dimensions

The first questions about fractals that we shall address is how to analyze them. The main tools of the trade come from measure theory and geometric measure theory in the form of measures and dimensions. Measures and dimensions are intimately tied together, and both give interesting information about a given fractal. In a very broad sense, a measure is just a way to assign a "size" to a set. It must be done in such a way that if we break down the set into a finite or countable number of pieces, the size of the whole set is the sum of the sizes of the pieces. A dimension, on the other hand, gives an idea as to how much space a set takes up near each of the points.

There are many ways to describe how much is in a set, and with fractals there are many different dimensions that we use to quantify how "large" the fractal is. We now list a few of these dimensions, and the measures that define them (when possible). Before we simply lay out the various dimensions, we first provide a discussion as to why these various forms are needed. We begin by looking at our familiar space $\mathbb{R}^n$. For this section, we follow the constructions described in [**10**].

1.2.1. Topological Dimension. In order to bring about a notion of *topological dimension, or Lebesgue covering dimension* (the definition of dimension that we are most familiar with from elementary math), we begin by looking at open covers of $\mathbb{R}^n$. Fix an open cover $\mathcal{U}$ of $\mathbb{R}^n$, and let $x \in \mathbb{R}^n$. We define the multiplicity of $\mathcal{U}$ at x, denoted $m(\mathcal{U}, x)$, as the number of sets in $\mathcal{U}$ that contain x. Next we define $m(\mathcal{U}) = \sup_x\{m(\mathcal{U}, x)\}$ as the multiplicity of $\mathcal{U}$. We could make this value as large as we want by adding in multiple copies of sets that cover x, so we are looking for the infimal value of $m(\mathcal{U})$. Therefore we define

$$m(\mathbb{R}^n) = \inf_{\mathcal{U}}\{m(\mathcal{U})\} \tag{1.2.1}$$

When $n = 1$, we can easily construct an open cover $\mathcal{U}$ of a line segment by two overlapping pieces, and thus $m(\mathcal{U}) = 2$. If these two elements of the cover did not overlap, then the line would be disconnected. Thus, this is also the infimal value and therefore $m(\mathbb{R}) = 2$. For $n = 2$, we can construct an optimal open cover using discs that has multiplicity 3 (see [**10**]). Thus, $m(\mathbb{R}^2) = 3$. Similarly, one can show that $m(\mathbb{R}^n) = n + 1$ for $n > 0$. This leads us to the following definition.

Definition 1.1. The *topological dimension (Lebesgue covering dimension)* of a topological space X is one less than the multiplicity of an optimal cover. That is, $\dim_T(X) = m(X) - 1$, where $m(X)$ is defined by (1.2.1). Following convention, define $\dim_T(\emptyset) = -1$.

Thus, we have arrived at our usual notion of dimension for common objects. That is, the topological dimension of a line is 1, of the plane is 2, etc. Therefore, we could think of measuring an object with $\dim_T(X) = 1$ by its length, measuring an object of $\dim_T(X) = 2$ by its area, $\dim_T(X) = 3$ by its volume, ... by using Lebesgue measure.

One thing to note is that by definition, the topological dimension will be an integer. For many sets this is fine, but with fractals we need a more robust definition. For example, we can take the Sierpinski Triangle as described in Example 1.1.2. The length of the perimeter from the original set to the first generation grows from length 3 to length 9/2. Since this process is repeated at each generation, the length of the perimeter grows according to $\left(\frac{3}{2}\right)^n$, which approaches infinity. So trying to measure the length of the fractal ends up with a value of infinity, which is not very helpful. One could then try measuring the area of the fractal, but we can see by the construction that the area grows according to $\left(\frac{3}{4}\right)^n$, which approaches zero. Thus the object is infinitely long but has zero area. Neither dimension 1 nor 2 gives us a good indication as to how much "stuff" is in the fractal or how much space it takes up. That is, we don't yet have a dimension for which measuring the fractal returns a useful value.

1.2.2. Hausdorff Measure and Dimension. It is clear that in order to achieve this specific dimension that will allow us to correctly measure the size of this object, we need to modify our definition of dimension. The topological dimension is too general to be able to take into account the fine detail of most fractals, and thus we need our definition of dimension to be dependent on a stronger property than just the number of covering sets. Thus, we will introduce a metric to our topological space, and define a measure using not just the number of pieces covering our set, but the size of those pieces.

In the following, let (X, d) be a metric space and $A \subseteq X$.

Definition 1.2. We say the collection $\mathcal{U} = \{U_i\}$ is a δ-cover of a set A if $A \subseteq \bigcup_i U_i$ and $\operatorname{diam}(U_i) \leq \delta$, where $\operatorname{diam}(U_i) = \sup\{d(x, y) \mid x, y \in U_i\}$.

Definition 1.3. Let A be a subset of a metric space X. Let $\delta > 0$, and $\mathcal{U} = \{U_i\}$ be a $\delta-$cover of A. For $s \in [0, \infty)$, define the s-dimensional content of $\mathcal{A}$ to be

$$H^s_\delta(A) = \inf_{\mathcal{U}} \left\{ \sum_{i=1}^{\infty} \operatorname{diam}(U_i)^s \mid \{U_i\} \text{ is a } \delta\text{-cover of } A \right\}, \tag{1.2.2}$$

where the infimum is taken over all δ-covers of A. Since the number of covers decreases as δ decreases, $H^s_\delta(A)$ is a monotonic function of δ. Thus a limit exists, and we define the s-dimensional Hausdorff measure to be

$$H^s(A) = \lim_{\delta \to 0} H^s_\delta(A). \tag{1.2.3}$$

Note that the definition of Hausdorff measure depends on the way we measure the diameter of the covering sets, and thus the metric itself.

An important note here is that we are using δ-covers of A, which can have sets with much smaller diameter than δ. As with the example of the Sierpinski triangle before, the size of the set could be ∞ or 0, but there can also be a specific value of s for which $0 < H^s(A) < \infty$. This specific value of s for which the measure changes from ∞ to 0 has the following two interesting properties.

PROPOSITION 1.4. *Suppose that $s \geq 0$ with $H^s(A) < \infty$. Then $H^t(A) = 0$ for all $t > s$.*

PROOF. Note that

$$\begin{aligned} H^t_\delta(A) &= \inf_{\mathcal{U}} \sum_i (\mathrm{diam}(U_i))^t \\ &= \inf_{\mathcal{U}} \sum_i (\mathrm{diam}(U_i))^{t-s} (\mathrm{diam}(U_i))^s \\ &\leq \inf_{\mathcal{U}} \sum_i \delta^{t-s} (\mathrm{diam}(U_i))^s \\ &= \delta^{t-s} H^s_\delta(A). \end{aligned}$$

Since $t - s > 0$, we know that $\delta^{t-s} \to 0$ as $\delta \to 0$. Since $H^s_\delta(A) \leq H^s(A) < \infty$, we have that $\lim_{\delta \to 0} H^t_\delta(A) = 0$. $\square$

As a consequence of this calculation, we also receive the following statement immediately.

PROPOSITION 1.5. *Suppose that $s \geq 0$ with $H^s(A) > 0$. Then $H^t(A) = \infty$ for all $s > t$.*

Finally, we define

$$\begin{aligned} \dim_H(A) &= \sup\{s \geq 0 \mid H^s(A) = \infty\} && (1.2.4) \\ &= \inf\{s \geq 0 \mid H^s(A) = 0\} && (1.2.5) \end{aligned}$$

to be the Hausdorff dimension of A.

From these two propositions, we can graph the set function $H^s(\cdot) : X \to [0, \infty) \cup \{\infty\}$.

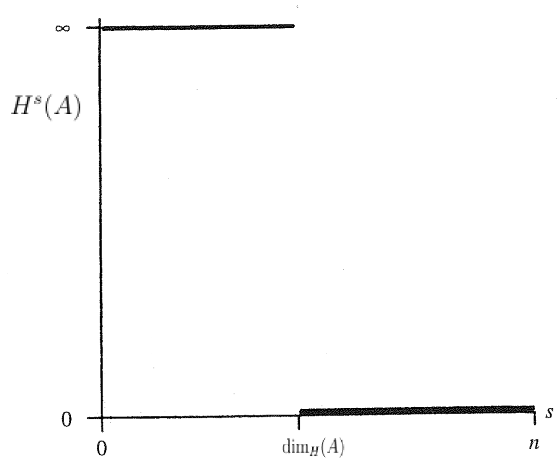

FIGURE 1.10. Graph of $H^s(A)$ versus s for a set A from [**12**].

1.2.3. Calculating Hausdorff Dimension. Often times our best attack to finding the Hausdorff dimension of a set is to find upper and lower bounds of $\dim_H$ and show that they coincide. Looking at the definition, we can see that in order to get an upper bound on the Hausdorff dimension, we need only find a single "good" open δ-cover to work with. The lower bound is generally much harder to find, requiring that we show that there is a lower bound for all open δ-covers. However, we can list a few immediate properties that will simplify some of our calculations. See [**12**] for proofs and more properties.

(1) $\dim_H \emptyset = 0$
(2) $\dim_H A \leq \dim_H B$ when $A \subseteq B$
(3) $\dim_H(\cup A_i) = \sup_i \dim_H A_i$ for any countable collection $\{A_i\}$ of subsets of $\mathbb{R}^n$.

Now that we have the definition of Hausdorff dimension under our belt, we want to see how this new notion of dimension meshes with our old topological definition. In particular, since $\dim_T(\mathbb{R}^n) = n$, we want to make sure that $\dim_H(\mathbb{R}^n) = n$ as well. To start, let's consider when $n = 1$.

PROPOSITION 1.6. *The Hausdorff dimension of the real line is 1, following property (3).*

PROOF. Let $A = [0,1] \subset \mathbb{R}$. It suffices to show that $\dim_H(A) = 1$.
Let $\delta > 0$. We will construct a cover of $[0,1]$ so that $\sum_i (\text{diam}(U_i))^1 \leq 3$, and thus we would have that $\dim_H(A) \leq 1$. Choose $n \in \mathbb{Z}$ such that $1/n \leq \delta$. For $i = 0, 1, \ldots, 3n-1$, consider the intervals $(i/3n, (i+1)/3n)$. These intervals cover everything in $[0,1]$ except the endpoints.

To construct U_i, we include three adjacent intervals with the i^{th} interval in the middle. Thus, $U_i = ((i-1)/3n, (i+2)/3n)$. Note that $\operatorname{diam}(U_i) = 1/n \leq \delta$ for each i. Thus, $\mathcal{U} = \{U_i\}_{i=0}^{3n-1}$ is a δ-cover of A. Therefore

$$\sum_i \operatorname{diam}(U_i) = 3n \cdot \frac{1}{n} = 3.$$

Thus, $\dim_H(A) \leq 1$.

The lower bound is much harder to achieve; a fact that is often the case when computing the dimension of a set. To start, fix $s < 1$. We now need to find a $\delta > 0$ such that for every δ-cover $\mathcal{U} = \{U_i\}$ of A, $\sum_i (\operatorname{diam}(U_i))^s > 1$. For such a $\mathcal{U}$, we would have

$$\sum_i (\operatorname{diam}(U_i))^s = \sum_i (\operatorname{diam}(U_i))(\operatorname{diam}(U_i))^{s-1} \geq \left(\sum_i \operatorname{diam}(U_i) \right) \delta^{s-1}.$$

Since $\mathcal{U}$ is a cover for $[0,1]$, we must have that $\sum_i \operatorname{diam}(U_i) \geq 1$. Thus, $\sum_i (\operatorname{diam}(U_i))^s \geq \delta^{s-1}$. Since $s < 1$, for sufficiently small δ we have $\delta^{s-1} > 1$. $\square$

So the Hausdorff dimension agrees with our intuitive topological dimension of $\mathbb{R}$. Following a similar but more general argument, one can show that $\dim_H(\mathbb{R}^n) = \dim_T(\mathbb{R}^n) = n$. In general, for a set $E \subseteq \mathbb{R}^n$,

$$\dim_T(E) \leq \dim_H(E). \tag{1.2.6}$$

In Mandelbrot's seminal paper [**25**], he originally defined a fractal to be a set where this inequality is strict. However, he began to move away from this definition as it was discovered that there are sets we would like to consider to be fractal that have equal Hausdorff and topological dimension (often pathologically constructed from existing fractals). Some consider a set to be a fractal if the inequality is strict and the Hausdorff dimension is not an integer, but we will stick with the bullet points from section 1. Later we will give a larger set of inequalities with a similar attempted definition.

1.2.4. Hausdorff Dimension and Metrics. Since we can equip a topological space with multiple metrics, one may ask what transformations happen to a fractal when we change the metric. Conversely, we can find what conditions are needed on the metric to make the dimension of the fractal invariant. Recall that two metrics d_1 and d_2 are *equivalent* if they induce the same topology. The topological dimension of a set will not change under two equivalent metrics because the definition only depends on the topology. However, this is not strong enough for Hausdorff dimension. Recall that two metrics d_1 and d_2 are *strongly equivalent* if there exists a positive constant C such that for all x, y in the space, we have

$$\frac{1}{C}d_2(x,y) \le d_1(x,y) \le Cd_2(x,y).$$

We can see from the definition of Hausdorff measure that if we pass to a strongly equivalent metric, the term $(\mathrm{diam}(U_i))^s$ changes by a factor of C. Thus, whether $H^s(A)$ is finite or infinite, $\dim_H(A)$ remains the same.

However, there is an interesting relationship between the topological dimension and Hausdorff dimension.

THEOREM 1.7 ([**10**]). *Given a set $A \subset \mathbb{R}^n$, the topological dimension is the infimum of all Hausdorff dimensions taken over all metrics ρ equivalent to the standard metric d. That is,*

$$\dim_T(A) = \inf_{\rho \sim d} \dim_H(A). \tag{1.2.7}$$

When calculating the Hausdorff dimension, we often get an upper bound for free by just considering the sets that make up the construction of a fractal as a cover of itself. As said before, when we calculate the upper bound for a fractal, we need only show that a specific cover is used. However, for the lower bound of the dimension, we must show sums of the form $\sum_i \mathrm{diam}(U_i)^s$ are greater than a positive constant for every δ-covering of A. This is a much more arduous task, as there are many such covers for a set. This means that we not only have to worry about the size of the sets in the construction, but also how far apart they are.

A simple method for finding a lower bound is to show that no individual set can cover too much of A compared to its own size, $\mathrm{diam}(U_i)^s$. Then by adding up all the covering sets $\{U_i\}$, their sum $\sum_i \mathrm{diam}(U_i)^s$ cannot be too small either. The common technique is to concentrate a mass distribution μ on A and compare $\mu(U_i)$ with $\mathrm{diam}(U_i)^s$.

THEOREM 1.8 (Mass distribution principle). *Let $A \subseteq \mathbb{R}^d$ and μ be a mass distribution (or probability measure) on A. Suppose that for some $s > 0$, there are numbers $c > 0$ and $\varepsilon > 0$ such* *that*

$$\mu(U) \leq c \cdot \operatorname{diam}(U)^s$$

for all μ-measurable sets U with $\operatorname{diam}(U) \leq \varepsilon$. *Then $\mathcal{H}^s(A) \geq \mu(A)/c$ and*

$$s \leq \dim_H(A).$$

PROOF. Let $\{U_i\}$ be a $\delta-$cover of A with $\delta < \varepsilon$. Then $A \subseteq \cup_i U_i$. Thus,

$$0 < \mu(A) \leq \mu\left(\bigcup_i U_i\right) \leq \sum_i \mu(U_i) \leq c \sum_i \operatorname{diam}(U_i)^s. \tag{1.2.8}$$

Thus, $0 < \mu(A)/c \leq \sum_i \operatorname{diam}(U_i)^s$. Taking the infimum of both sides, we have that $\mu(A)/c \leq \mathcal{H}^s_\delta(A)$ for small enough δ. Taking $\delta \to 0$, we get $\mu(A)/c \leq \mathcal{H}^s(A)$. Since μ is concentrated on A, $\mu(A) > 0$, and thus $\dim_H(A) \geq s$. $\square$

The Mass distribution principle is especially helpful in calculating a lower bound for the Hausdorff dimension. The measure used in the Mass Distribution Principle is usually chosen to be uniform across the fractal. There is an analog for a non-uniform distribution, however it is a little more technical.

DEFINITION 1.9. Suppose μ is a finite measure on $\mathbb{R}^n$, $E \subseteq \mathbb{R}^n$, and $x \in E$. Define the pointwise dimension of μ at x as

$$\dim_\mu(x) = \lim_{r \to 0} \frac{\log(\mu(B(x,r)))}{\log(r)} \tag{1.2.9}$$

if the limit exists. We can also define $\underline{\dim}_\mu(x)$ and $\overline{\dim}_\mu(x)$ in the usual way for the lower and upper pointwise dimensions of μ at x.

Something to note is that this definition of dimension is not a property of the set, but of the measure. Note also that this limit may not exist for each $x \in \mathbb{R}^n$.

THEOREM 1.10 (Non-uniform Mass Distribution Principle, [**10**]). *If μ is a finite measure on $\mathbb{R}^n$, $E \subset \mathbb{R}^n$ with $\mu(E) > 0$, and there exists $\alpha > 0$ such that $\underline{\dim}_\mu(x) \geq \alpha$ for $\mu-$almost every $x \in E$, then* $\dim_H(E) \geq \alpha$.

1.2.5. Hausdorff Dimension under Mappings. A natural question to ask is what will happen to the dimension if the set in question is mapped under various types of functions (continuous, Lipschitz, affinities, ...). That is, we want to compare the dimensions of A with $f(A)$. To start, suppose f is a continuous function on A. For example, if f is a projection to a subspace, then $\dim_H(f(A)) < \dim_H(A)$ for a suitably chosen A. However, there are continuous space filling curves that can take a set with Hausdorff dimension 1 to a set with dimension 2. Thus continuous functions are too general to be able to say what happens to the dimension of their images.

However, Lipschitz functions act nicely with Hausdorff dimension. We first prove a stronger statement than we need involving Hölder continuous functions.

Proposition 1.11. *Let X, Y be metric spaces and $A \subseteq X$. If $f : X \to Y$ satisfies $d_Y(f(x), f(y)) \leq c d_X(x, y)^\alpha$ for all $x, y \in X$ and constants $\alpha > 0$ and $c > 0$, then for each s we have $H^{s/\alpha}(f(A)) \leq c^{s/\alpha} H^s(A)$, and $\dim_H(f(A)) \leq \frac{1}{\alpha} \dim_H(A)$.*

Proof. Let $\mathcal{U} = \{U_i\}$ be any δ-cover of A. Then

$$\operatorname{diam}(f(A \cap U_i)) \leq c\operatorname{diam}(A \cap U_i)^\alpha \leq c\operatorname{diam}(U_i)^\alpha, \tag{1.2.10}$$

so $f(A \cap \mathcal{U}) = \{f(X \cap U_i)\}$ is a $c\delta^\alpha$-cover of $f(A)$. Thus, we have

$$\sum_i (\operatorname{diam}(f(A \cap U_i))^{s/\alpha} \leq c^{s/\alpha} \sum_i (\operatorname{diam}(U_i))^s.$$

Hence, we have $H^{s/\alpha}_{c\delta^\alpha}(f(A)) \leq c^{s/\alpha} H^s_\delta(A)$. Taking limits as before, $H^{s/\alpha}(f(A)) \leq c^{s/\alpha} H^{s/\alpha}(A)$. To prove the result for the dimension, suppose $s > \dim_H(A)$. By Proposition 1.4 and the above, $H^{s/\alpha}(f(A)) \leq c^{s/\alpha} H^s(A) = 0$. Thus, $\dim_H(f(A)) \leq s/\alpha$ for each $s > \dim_H(A)$. $\square$

Setting $\alpha = 1$ in the previous proposition immediately gives us the results for Lipschitz functions.

Corollary 1.12. *If $f : A \to \mathbb{R}^n$ is Lipschitz, then for every $A \subseteq \mathbb{R}^n$, we have $\dim_H(f(A)) \leq \dim_H(A)$.*

If our functions are even more controlled, e.g. bi-Lipschitz, then the dimension of the image is invariant.

Proposition 1.13. *If* $f : A \to \mathbb{R}^n$ *is a bi-Lipschitz map, then* $\dim_H(f(A)) = \dim_H(A)$.

Proof. We can apply the Lipschitz result to $f^{-1} : f(A) \to A$ to get the reverse inequality $\dim_H(A) \leq \dim_H(f(A))$. $\square$

Therefore bi-Lipschitz mappings will act as the invariant transformations of metric spaces (and thus fractals), just as homeomorphisms do for topological spaces.

1.3. Other Notions of Dimension

1.3.1. Box Dimension. Since it seems that Hausdorff measure (and dimension) can be a pain to compute (even for a nice set like $\mathbb{R}$), we present some other definitions of dimension and discuss how they relate to the topological and Hausdorff dimensions. To start, we ask the question: what if we restricted ourselves to covering sets that have exactly diameter δ instead of diameter at most δ?

Let A be a subset of $\mathbb{R}^n$. Define the function

$$B^s_\delta(A) = \inf_{\mathcal{U}} \left\{ \sum_{i=1}^{\infty} \operatorname{diam}(U_i)^s \mid U_i \text{ open}, A \subseteq \bigcup_i U_i, \operatorname{diam}(U_i) = \delta \right\}. \tag{1.3.1}$$

The only difference between this equation and that for Hausdorff in (1.2.2) is that we require equality of the diameters of the cover sets. This seemingly small change has drastic consequences. The first is that we are no longer guaranteed a limit as $\delta \to 0$ since two different values of δ results in two disjoint collections of covers. Thus, we can only define an upper and lower limit

$$\overline{B}^s(A) = \limsup_{\delta \to 0} B^s_\delta(A), \tag{1.3.2}$$

$$\underline{B}^s(A) = \liminf_{\delta \to 0} B^s_\delta(A). \tag{1.3.3}$$

Note here that neither $\overline{B}^s$ nor $\underline{B}^s$ is a measure. As with Hausdorff dimension, we can list a few immediate properties:

(1) $\overline{B}^s(\emptyset) = \underline{B}^s(\emptyset) = 0$.
(2) $\overline{B}^s(U) \leq \overline{B}^s(V)$ and $\underline{B}^s(U) \leq \underline{B}^s(V)$ when $U \subseteq V$.

We remark that there is a noticeable lack of a third condition compared with the properties of Hausdorff measure (3). Since the proof of sub-additivity for Hausdorff dimension requires sets of continually small diameter, we cannot apply the same argument here. In fact, the only result we can manage to squeeze out is that $\overline{B}^s$ is sub-additive on finite collections U, but there is no such result for $\underline{B}^s$.

There is still the same sort of behavior as in Hausdorff dimension, with a specific value of s for which $\overline{B}^s(A)$ jumps from ∞ to 0 (similarly for $\underline{B}^s(A)$). From this, we can define the upper box dimension and lower box dimension as

$$\begin{aligned}
\underline{\dim}_B(A) &= \sup\{s > 0 \mid \underline{B}^s(A) = \infty\} && (1.3.4)\\
&= \inf\{s > 0 \mid \underline{B}^s(A) = 0\} && (1.3.5)\\
\overline{\dim}_B(A) &= \sup\{s > 0 \mid \overline{B}^s(A) = \infty\} && (1.3.6)\\
&= \inf\{s > 0 \mid \overline{B}^s(A) = 0\}. && (1.3.7)
\end{aligned}$$

An equivalent way to describe the box dimension is the following.

Definition 1.14. Let $N_\delta(A)$ denote the minimum number of δ-balls centered in A required to cover A. The lower box dimension and upper box dimension of A, are the infimal value of s for which there exists a constant K such that for any $0 < \delta < 1$,

$$N_\delta(A) \leq K(1/\delta)^s.$$

In other words,

$$\begin{aligned}
\underline{\dim}_B(A) &= \liminf_{\delta \to 0} \frac{\log(N_\delta(A))}{-\log(\delta)}, && (1.3.8)\\
\overline{\dim}_B(A) &= \limsup_{\delta \to 0} \frac{\log(N_\delta(A))}{-\log(\delta)}. && (1.3.9)
\end{aligned}$$

Note here that for these limits to make sense, $N_\delta(A)$ must be finite, and A must be a bounded set.

Proposition 1.15. *For $A \subseteq \mathbb{R}^n$, both the upper (and lower) box dimension of A is equal to the upper (or lower respectively) box dimension of the closure of A.*

Because of this proposition, we actually need only consider compact subsets of $\mathbb{R}^n$ for the box dimension.

EXAMPLE 1.3.1. A feature of box dimension is that sets we would normally consider to be "small", like countably infinite, can still have full dimension. Consider the set of rational numbers in $[0,1]$, $A = \mathbb{Q} \cap [0,1]$. We would like to consider this set as "small" because it is countable, and yet because it is dense in $[0,1]$, $\dim_B(A) = 1$. In a definition of dimension that depends on a measure, small sets would not have the same dimension as the ambient space. Even though Proposition 1.15 could be seen as a drawback, the box dimension is often used to great effect with computers to get a rough estimate of a dimension for a given fractal or set.

However, the box dimension does share some properties with Hausdorff dimension. For example, under Lipschitz and bi-Lipschitz maps we have similar results.

PROPOSITION 1.16. *If $f : \mathbb{R}^n \to \mathbb{R}^n$ is Lipschitz, then for every $A \subseteq \mathbb{R}^n$, $\underline{\dim}_B(f(A)) \leq \underline{\dim}_B(A)$ and $\overline{\dim}_B(f(A)) \leq \overline{\dim}_B(A)$.*

COROLLARY 1.17. *If f is bi-Lipschitz then $\underline{\dim}_B(f(A)) = \underline{\dim}_B(A)$ and $\overline{\dim}_B(f(A)) \leq \overline{\dim}_B(A)$.*

The relationship between Hausdorff and box dimension is given by

$$\dim_H(A) \leq \underline{\dim}_B(A) \leq \overline{\dim}_B(A). \tag{1.3.10}$$

The inequalities here can be strict. Here we give an example from [**10**] in order to illustrate how even a simple subset of $[0,1]$ that converges to zero can be constructed to make each inequality strict.

EXAMPLE 1.3.2 ([**10**]). Given any $0 < \alpha \leq \beta < 1$, there exists a countable closed set $A \subset [0,1]$ such that $\dim_H(A) = 0, \underline{\dim}_B(A) = \alpha, \overline{\dim}_B(A) = \beta$. Fix $0 < a \leq 1/3$, and consider the sequence $a_n = a^n$ which converges to zero. We will construct a set $A \subset [0,1]$ as an increasing sequence beginning at 0; the first terms will be separated by a gap of length a_1, the next few by a gap of length a_2, and so on. That is, the set A will be the sequence

(1.3.11)

$$\Big\{0, a_1, 2a_1, \dots, b_1a_1,$$

$$b_1a_1 + a_2, b_1a_1 + 2a_2, \dots, b_1a_1 + b_2a_2,$$

$$\vdots$$

$$\left(\sum_{k=1}^{n} b_ka_k\right) + a_{n+1}, \dots, \left(\sum_{k=1}^{n} b_ka_k\right) + b_{n+1}a_{n+1},$$

$$\left(\sum_{k=1}^{n+1} b_ka_k\right) + a_{n+2}, \dots\Big\}$$

together with its limit point, where (b_n) is a sequence of nonnegative integers which we will choose so as to obtain the desired result for the lower and upper box dimensions. We write the endpoints between sequences of differently spaced points as

$$T_n = \sum_{k=1}^{n} b_ka_k, \tag{1.3.12}$$

and see that $\lim_{n\to\infty} T_n = T$, the limit point of A.

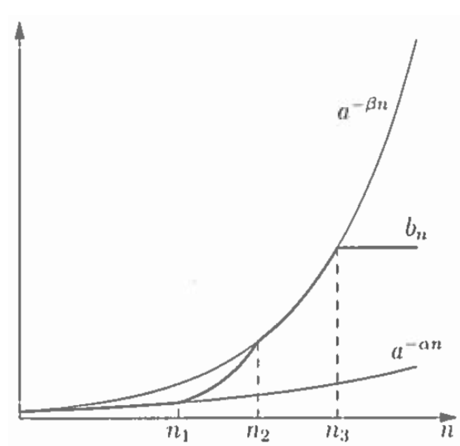

Figure 1.11. Constructing the sequence b_n

The fact that $\dim_H(A) = 0$ follows immediately from the fact that A is countable, and so it remains to choose (b_n) so as to guarantee $\underline{\dim}_B(A) = \alpha$ and $\overline{\dim}_B(A) = \beta$. The key properties of our sequence (b_n) will be as follows:

(1) (b_n) tends to infinity monotonically as $n \to \infty$.

(2) $\sum_{n=1}^{\infty} a_n b_n < 1$.

(3) The exponential growth rate of the partial sums $S_n = \sum_{k=1}^{n} b_k$ is given by

$$\liminf_{n\to\infty} \frac{\log(S_n)}{-\log(a_n)} = \alpha, \qquad \limsup_{n\to\infty} \frac{\log(S_n)}{-\log(a_n)} = \beta.$$

(4) The "tail" $[T_n, T]$ of the set A is not too long: there exists a constant C such that

$$\frac{T - T_n}{a_n S_n} \leq C$$

for all n.

Property (2) guarantees that A is bounded. The significance of the partial sums S_n is that they let us estimate $N_\varepsilon(A)$, the cardinality of an optimal cover by open sets of diameter ϵ. Indeed, for $\epsilon = a^n$, we see that any such cover must contain at least S_n sets, since each set can contain at most one of the points $T_k + ma_k$ for $k \leq n$, $m \leq b_k$, and S_n is the number of such points. Furthermore, we may cover the interval $[T_n, T]$ with $(T - T_n)/\epsilon$ intervals of length ϵ, and by property (4), this shows that $N_\varepsilon(A) \leq (C + 1)/S_n$. The result for the lower and upper box dimensions will then follow immediately from property (3).

It remains only to produce a sequence with these properties. To this end, we follow a four-step recursive procedure, illustrated in the Figure 1.11. At first, b_n is just the integer part of $a^{-\alpha n}$, and so S_n also grows at the same rate as $a^{-\alpha n}$. It follows that the quantity $\log(S_n)/\log(1/a_n)$ converges to α as n grows, and so we may choose n_1 such that

$$\left| \frac{\log(S_{n_1})}{\log(1/a_{n_1})} - \alpha \right| < \frac{1}{2}. \tag{1.3.13}$$

Now we would like to let b_n follow the function $a^{-\beta n}$ for a while, to approximate the desired upper limit, but if we jump directly to the graph of $a^{-\beta n}$ at n_1, we will find that the sequence we eventually produce fails property (4), and so we must be slightly more careful. Thus, for $n > n_1$, we let b_n

grow exponentially until it reaches the upper function at n_2, at which point we have b_n follow $a^{-\beta n}$ until

$$\left|\frac{\log(S_{n_3})}{\log(1/a_{n_3})} - \alpha\right| < \frac{1}{2}. \tag{1.3.14}$$

Finally, for $n > n_3$, we leave b_n constant until it is once again equal to $a^{-\alpha n}$ at n_4 (which is somewhere off the right edge of the graph in Figure 1.11). Then we iterate all four steps of this procedure, replacing the bound 1/2 in (1.3.13) and (1.3.14) with $(1/2)^k$ at the k^{th} iteration. One may then verify that the sequence (b_n) so constructed has properties (1)−(4), ad thus the set A given in (1.3.11) has the dimensions claimed.

Since box dimension also relies on the metric, there is an analog to Theorem 1.7 for general subsets $E \subseteq R^n$ published by Pontryagin and Schnirel'man in 1932.

THEOREM 1.18 ([**33**]). *Let $E \subseteq \mathbb{R}^n$. The topological dimension is the infimum of all possible lower box dimensions taken over all metrics ρ equivalent to the standard metric d. That is,*

$$\dim_T(E) = \inf_{\rho\sim d} \underline{\dim}_B(E). \tag{1.3.15}$$

Pontryagin and Shnirel'man showed also that there is no similar result for the upper box dimension.

1.3.2. Assouad Dimension. In 1977, Patrice Assouad defined a new generalization of the box dimension in his PhD thesis, [**1**]. This new definition of dimension has become a very active research area of late.

DEFINITION 1.19. Let $N_{r,\delta}(A)$ denote the number of δ-balls centered in A required to cover any r-ball centered in A. The Assouad dimension of A, denoted $\dim_A(A)$, is the infimal value of s for which there exists a constant K such that for any $0 < \delta < r < 1$,

$$N_{r,\delta}(A) \leq K(r/\delta)^s.$$

With this definition, we now have a new chain of dimensional inequalities from [**14**]:

$$\dim_T(E) \le \dim_H(E) \le \underline{\dim}_B(E) \le \overline{\dim}_B(E) \le \dim_A(E) \tag{1.3.16}$$

We briefly return to the question: what makes a set a fractal? Some consider a set to be a fractal if any one of the inequalities in (1.3.16) above are strict. With this definition we run into a similar issue as Mandelbrot, namely that this would include sets that we wouldn't generally think of as fractal, or excludes sets that should be considered fractal.

Example 1.3.3. Let $E = \{1/n\}_{n=1}^{\infty} \cup \{0\} \subseteq \mathbb{R}$. Then

(1) $\dim_T(E) = \dim_H(E) = 0$,
(2) $\dim_B(E) = \frac{1}{2}$,
(3) $\dim_A(E) = 1$.

Proof. Note that (1) is rather trivial since E is a countable collection of points. For (2), we show the calculation made in [**12**]. Let $0 < \delta < 1/2$ and let k be the integer satisfying

$$\frac{1}{k(k+1)} \le \delta < \frac{1}{(k-1)k}.$$

If $\operatorname{diam}(U) \le \delta$, then U can cover at most one of the points $\{1, \frac{1}{2}, \ldots, \frac{1}{k}\}$ since the distance between any pair of these points is at least

$$\frac{1}{k-1} - \frac{1}{k} = \frac{1}{(k-1)k} > \delta.$$

Thus, at least k sets of diameter δ are required to cover E, so $N_\delta(ES) \ge k$ giving

$$\frac{\log(N_\delta(E))}{-\log(\delta)} \ge \frac{\log(k)}{\log(k(k+1))} = \frac{\log(k)}{2\log(k) + \log(1+\frac{1}{k})} \to \frac{1}{2} \tag{1.3.17}$$

as $k \to \infty$ corresponding to $\delta \to 0$, so $\underline{\dim}_B(E) \ge \frac{1}{2}$.

On the other hand, since $\delta \ge \dfrac{1}{k(k+1)}$, $k+1$ intervals of length δ cover $[0, 1/k]$, leaving $k-1$ points of E which can be covered by another $k-1$ intervals. Thus, $N_\delta(E) \le 2k$, so

$$\frac{\log(N_\delta(E))}{-\log(\delta)} \le \frac{\log(2k)}{\log(k(k-1))} = \frac{\log(2) + \log(k)}{2\log(k) + \log(1-\frac{1}{k})} \to \frac{1}{2} \tag{1.3.18}$$

on taking the limit, giving $\overline{\dim}_B(F) \le \frac{1}{2}$.

For (3), see [**9**], Lemma 3.1. $\square$

1.3.3. Packing Dimension. The last notion of a dimension that we will mention here is usually considered to be the dual of Hausdorff dimension. Hausdorff dimension is defined by using good coverings by small balls, and in what follows we will construct a dimension using packings of large collections of small disjoint balls with centers in the set.

DEFINITION 1.20. Let $A \neq \emptyset$ be a bounded subset of $\mathbb{R}^d$. For any $s > 0$, we define

$$P^s_{0,\delta}(A) = \sup\left\{\sum_{i=1}^{\infty} \operatorname{diam}(U_i)^s \mid \{U_i\} \text{ is a collection of disjoint balls of radii at most } \delta \text{ with centers in } A\right\}.$$

Next, we have that

$$P^s_0(A) = \lim_{\delta\to 0} P^s_{0,\delta}(A),$$

since $P^s_{0,\delta}(A)$ decreases as δ decreases. Then the s-dimensional packing measure of A is defined by

$$P^s(A) = \inf\left\{\sum_{i=1}^{\infty} P^s_0(U_i) \mid A \subseteq \bigcup_{i=1}^{\infty} U_i\right\}.$$

The packing dimension of A, denoted $\dim_P(A)$, is defined by

$$\dim_P(A) = \sup\{s \mid P^s(A) = \infty\} \tag{1.3.19}$$

$$= \inf\{s \mid P^s(A) = 0\} \tag{1.3.20}$$

PROPOSITION 1.21 ([**14**]). *If A is compact, then*

$$\dim_T(A) \le \dim_H(A) \le \dim_P(A) \le \overline{\dim}_B(A) \le \dim_A(A) \tag{1.3.21}$$

For suitably chosen A, any of these inequalities can be strict.

CHAPTER 2

Moran Sets and Iterated Function Systems

Now that we have the proper measures and dimensions to study fractals, we need ways to create the fractals themselves. In this chapter we will describe two of the most popular and common ways to create fractals: one that follows a more geometric approach like von Koch, and the other a more analytic approach like Fatou and Julia.

2.1. Moran Sets

The classic construction of Moran sets was introduced in [**29**]. We reproduce the definition here with a more current interpretation to introduce notations.

Let $\{n_k\}_{k\geq 1}$ be a sequence of positive integers for $k \geq 1$. Here k will represent the generation, and n_k will be the number of children in generation k that each parent set from generation $k-1$ has. For any $k \in \mathbb{N}$, define

$$D_k = \{(i_1, i_2, \cdots, i_k) : 1 \leq i_j \leq n_k, 1 \leq j \leq k\} \text{ and } D = \bigcup_{k\geq 0} D_k \text{ with } D_0 = \emptyset \tag{2.1.1}$$

Let $\sigma = (\sigma_1, \cdots, \sigma_k) \in D_k$ and $\tau = (\tau_1, \cdots, \tau_m) \in D_m$, then denote

$$\sigma * \tau = (\sigma_1, \cdots, \sigma_k, \tau_1, \cdots, \tau_m) \in D_{k+m}. \tag{2.1.2}$$

Using this notation, we may express

$$D_k = \{\sigma * j \mid \sigma \in D_{k-1}, 1 \leq j \leq n_k\} \tag{2.1.3}$$

to emphasize the process of moving between generations.

Suppose $\mathcal{J} := \{J_\sigma : \sigma \in D\}$ is a collection of subsets of $\mathbb{R}^N$. Set

$$E_k = \bigcup_{\sigma \in D_k} J_\sigma, \text{ and } F = \bigcap_{k\geq 0} E_k. \tag{2.1.4}$$

We call F the limit set associated with the collection $\mathcal{J}$.

Definition 2.1 ([**18**]). Suppose that $J \subset \mathbb{R}^N$ is a compact set with nonempty interior. Let $\{n_k\}_{k\geq 1}$ be a sequence of positive integers, and $\{\Phi_k\}_{k\geq 1}$ be a sequence of positive real vectors with

$$\Phi_k = (c_{k,1}, c_{k,2}, \ldots, c_{k,n_k}), \sum_{1\leq j\leq n_k} c_{k,j} \leq 1, k \in \mathbb{N}. \tag{2.1.5}$$

Suppose that $\mathcal{F} := \{J_\sigma : \sigma \in D\}$ is a collection of subsets of $\mathbb{R}^N$, where D is given in (2.1.1). We say that the collection $\mathcal{F}$ fulfills the Moran Structure provided it satisfies the following Moran Structure Conditions (MSC):

MSC(1) $J_\emptyset = J$.

MSC(2) For any $\sigma \in D$, J_σ is geometrically similar to J. That is, there exists a similarity $S_\sigma : \mathbb{R}^N \to \mathbb{R}^N$ such that $J_\sigma = S_\sigma(J)$.

MSC(3) For any $k \geq 0$ and $\sigma \in D_k$, $J_{\sigma\star 1}, \ldots, J_{\sigma\star n_k}$ are subsets of J_σ, and $int(J_{\sigma\star i}) \cap int(J_{\sigma\star j}) = \emptyset$ for $i \neq j$.

MSC(4) For any $k \geq 1$ and $\sigma \in D_{k-1}, 1 \leq j \leq n_k$,

$$\frac{diam(J_{\sigma\star j})}{diam(J_\sigma)} = c_{k,j}. \tag{2.1.6}$$

For the collection $\mathcal{F}$ fulfilling the MSC, the limit set F given in (2.1.4) is a nonempty compact set. This limit set F is called the Moran set associated with the collection $\mathcal{F}$. This Moran set is self-similar, and has been studied extensively by many authors with various approaches (e.g. [**29**], [**19**], [**12**], [**7**], [**31**]).

Example 2.1.1. Notice that the Cantor set in Example 1.1.1 is a Moran set. The Cantor set has $n_k = 2$ and $\Phi_k = \{(1/3, 1/3)\}$ for all $k > 0$.

Example 2.1.2. Here we give an example of the first few generations of a Moran set constructed from intervals. In this example, we choose $n_k = \{2, 3, 2, \ldots\}$ and $\{\Phi_k\} = \{(6/10, 2/10), (1/12, 1/3, 1/6), (1/10, 3/4), \ldots\}$, with initial set $J_\emptyset = [0, 1]$. See Figure 2.1. Notice that the placements of the subsets varies within the parent sets for each generation, while sometimes the endpoints match up, and sometimes they do not.

FIGURE 2.1. First four generations of a Moran construction

The fact that there are four conditions to create a Moran set makes the area ripe for generalizations or restrictions. Note that in condition MSC(2), the sets in the new generation are geometrically similar, which is a rather strong condition. In MSC(3) the interiors of the next generation may not overlap, but says nothing else of the spacing between these sets. Condition MSC(4) requires that the sets in the new generation all have the same pattern of ratios for each iteration. There is even a hidden condition in MSC(2) that one may want to do away with in that the locations of the sets $J_{\sigma * j}$ are completely determined by the similarities used on J_σ. Here we discuss some of the many generalizations and restrictions that have been studied.

Often times in the literature one may define a self-similar set (SSS), E, to be a set satisfying the MSC as well as the fact that the set of similarities $\{S_\sigma\}$ has finite cardinality, the ratios described in MSC(4) do not change over generations (i.e. $c_{k,j} = c_j$), and that the system is deterministic. In this case, the dimensions of the Moran set are known to coincide $\dim_H = \underline{\dim}_B = \overline{\dim}_B = \dim_P$, see [**18**]. However, the dimensions may differ when we begin to modify the MSC.

There are many generalizations for MSC(2). For a SSS, E, one could change MSC(2) to use conformal maps instead of similarities. The resulting set is called a cookie-cutter set, and has been studied by Bedford in [**8**]. Alternatively, one could use affine maps, as studied by McMullen in [**28**]. In this setting, however, calculations of the dimension of limit sets can become particularly difficult. One could also study the limit sets generated by infinitely many similarities, as in [**26**]. In [**23**], the authors removed MSC(2), but required $\overline{int(J_\sigma)} = J_\sigma$ in their construction, and studied the dimension of the resulting fractals. In [**17**], Holland and Zhang studied a construction that replaced similarity maps in MSC(2) with a more general class of functions that are not necessarily contractions. In [**32**], Pesin and Weiss removed the requirement for similarities from MSC(2), but also relaxed MSC(3) from non-intersecting basic sets to non-intersecting balls contained in the basic sets. In particular they pursued sufficient conditions for which the box dimension and Hausdorff dimensions coincide. For more examples of modifications to the Moran set definition, see [**18**], [**38**] and the references therein.

With each modification to the MSC, one seems to find a new name for the limit set. As stated above, cookie-cutter sets come from conformal functions replacing the similarities in MSC(2) of an SSS ([**24**], [**8**]). There are Cantor-like sets [**22**], homogeneous and inhomogeneous Moran sets [**17**], generalized moran sets [**23**], controlled and weakly controlled Moran sets [**34**], deterministic and random Moran sets [**32**], parabolic cantor sets [**37**], graph directed constructions [**27**], etc

The fact that the placements of the subsets in a new generation can be arbitrary means calculating the dimension of a Moran set can be very tricky. Often times the way to get a handle on the Hausdorff dimension of Moran sets is through the use of nets and net measures, as in [**18**]. For calculations of the Assouad dimension of Moran sets, see [**21**].

2.2. Iterated Function Systems

One of the most important observations of Julia and Fatou was that one could determine information about the shape and geometry of an attractor from the functions used to create it. Since computers were not invented yet, they did not have the tools to fully realize what the geometry of the objects they were creating looked like visually. They also were focused on iterations of a single map in the complex plane. In this section we will see a specific form of Moran set, and pay more attention to the maps that are used to generate it.

Many fractals are self-similar, including the fractals mentioned in Chapter 1 (the Cantor set, the Sierpinski triangle, and the Menger sponge are all self-similar fractals). This property seemed to be intrinsic to the construction process of the fractals, and we can make that more formal. By using a formal process to guarantee a self-similar set, we often also make calculating the dimension much easier.

Let Δ be a closed subset of a metric space (X, d). Recall that a map $S : \Delta \to \Delta$ is a *contraction* on Δ if there exists a number $0 < c < 1$ such that $d(S(x), S(y)) \leq cd(x, y)$ for all $x, y \in \Delta$. If we have equality, that is, $d(S(x), S(y)) = cd(x, y)$, then we call S a *similarity*.

DEFINITION 2.2. An Iterated Function System (IFS) is a collection $S = \{S_1, S_2, \ldots, S_m\}$ of two or more continuous maps on $\mathbb{R}^d$ such that for each i, there exists $c_i \in (0, 1)$ such that $\|S_i(x) - S_i(y)\| \leq c_i \|x - y\|$ for all $x, y \in \mathbb{R}^d$. The constant c_i is called the contraction ratio of S_i.

In 1981, Hutchinson gave a generalization of Banach's Contraction Mapping Theorem from one contracting function to finitely many.

THEOREM 2.3 ([**19**]). *If $S = \{S_1, \ldots, S_m\}$ is an IFS, and S_i is a contraction with contraction ratio c_i for $i = 1, \ldots, m$, then there exists a unique, non-empty, compact set A such that*

$$A = \bigcup_{i=1}^{m} S_i(A). \tag{2.2.1}$$

This set is called the attractor of S.

PROOF. Let $\mathcal{S}$ be the set of all non-empty compact subsets of Δ. Let A_δ be the δ-neighborhood of a set $A \in \mathcal{S}$. We equip $\mathcal{S}$ with the Hausdorff metric

$$d_H(A, B) := \inf\{\delta \mid A \subset B_\delta \text{ and } B \subset A_\delta\}.$$

Then $(\mathcal{S}, d_H)$ forms a complete metric space.
For $E \in \mathcal{S}$, define $S : \mathcal{S} \to \mathcal{S}$ by

$$S(E) = \bigcup_{i=1}^{m} S_i(E). \tag{2.2.2}$$

Let $A, B \in \mathcal{S}$. Note that if $S_i(B) \subseteq (S_i(A))_\delta$ for all i, then $\cup_{i=1}^{m} S_i(B) \subseteq (\cup_{i=1}^{m} S_i(A))_\delta$. Thus,

$$d_H(S(A), S(B)) = d_H\left(\bigcup_{i=1}^{m} S_i(A), \bigcup_{i=1}^{m} S_i(B)\right) \leq \max_{1 \leq i \leq m} d_H(S_i(A), S_i(B)). \tag{2.2.3}$$

Since each S_i is a contraction, we have that

$$d_H(S(A), S(B)) \leq (\max_{1\leq i\leq m} c_i) d(A, B). \tag{2.2.4}$$

Since $0 < \max_{1\leq i\leq m} c_i < 1$, we have that S is a contraction on $(\mathcal{S}, d)$. Since $(\mathcal{S}, d)$ is complete, by the Contraction Mapping Theorem, S has a unique fixed point $A \in \mathcal{S}$ such that $S(A) = A$. In fact, if we can assume that $S_i(E) \subseteq E$ for all i, then $S(E) \subseteq E$. Thus, iteratively applying S to its own image results in a sequence of nested non-empty compacts sets and the distance between the k^{th} iterate of S and A decreases to zero as k tends to infinity. Thus,

$$A = \bigcap_{k=0}^{\infty} \bigcup_{i=1}^{m} S_i(E) \tag{2.2.5}$$

for every non-empty compact subset $E \in \mathcal{S}$. □

One would normally see this definition and like to call A the invariant set of the IFS $\{S_1, \ldots, S_m\}$, which would not be wrong. However, because Hutchinson was working from a dynamical systems point of view, it is customary to use the nomenclature of that discipline instead.

If one started with a given set, how would we know if the attractor of an IFS is close to approximating the set? The following theorem, known as the Collage Theorem, gives such an estimate.

Theorem 2.4 (Collage Theorem, [**12**]). *Let $\{S_1, \ldots, S_m\}$ be an IFS on $\Delta \subset \mathbb{R}^n$ and suppose that $||S_i(x) - S_i(y)|| \leq c||x - y||$ for all $x, y \in \mathbb{R}^n$ and all i, where $c < 1$. Let $E \subseteq \Delta$ be any non-empty compact set. Then*

$$d_H(E, A) \leq \frac{1}{1-c} d_H\left(E, \bigcup_{i=1}^{m} S_i(E)\right), \tag{2.2.6}$$

where A is the attractor for the IFS and d_H is the Hausdorff metric.

The corollay to this theorem shows that essentially any set can be approximated arbitrarily closely by an attractor from an IFS.

Corollary 2.5 ([**12**]). *Let E be a non-empty compact subset of $\mathbb{R}^n$. Given $\delta > 0$, there exists IFS of similarities $\{S_1, \ldots, S_m\}$ with attractor A satisfying $d_H(E, A) < \delta$.*

PROOF. Let $\delta > 0$. Let $B_1, \ldots, B_m$ be a collection of balls that cover E whose centers are in E and have radii less than of equal to $\delta/4$. Then $E \subseteq \cup_{i=1}^m B_i \subseteq E_{\delta/4}$, where $E_{\delta/4}$ is the $\delta/4-$neighborhood of E. For each $i = 1, \ldots m$, let S_i be any contracting similarity such that $c_i < 1/2$ and $S_i(E) \subseteq B_i$. Thus $S_i(E) \subset B_i \subseteq (S_i(E))_{\delta/2}$, and so

$$\left(\bigcup_{i=1}^{m} S_i(E)\right) \subseteq E_{\delta/4} \text{ and } E \subseteq \bigcup_{i=1}^{m} (S_i(E))_{\delta/2}. \tag{2.2.7}$$

Then by the definition of the Hausdorff metric, $d_H(E, \cup_{i=1}^m S_i(E)) \leq \delta/2$. Therefore, by (2.2.6),

$$d_H(E, A) \leq 2 \cdot d_H(E, \cup_{i=1}^m S_i(E)) \leq \delta \tag{2.2.8}$$

where A is the attractor of $\{S_1, \ldots, S_m\}$. □

The problem with this corollary is that the IFS may have a very large amount of similarities in it, making the IFS rather unwiedly to actually use in practice. However, the corollary is often used in conjunction with some observations about the self-similarity of the set in order to reduce m to something more manageable.

In order to make sure that the images of the similarities in an IFS do not overlap too much, we can define the following condition.

DEFINITION 2.6. An IFS $S = \{S_i\}_{i=1}^m$ is said to satisfy the Open Set Condition (OSC) if there exists a non-empty open set U such that $\bigcup_{i=1}^m S_i(U) \subseteq U$, and $S_i(U) \cap S_j(U) = \emptyset$ whenever $i \neq j$.

As shown in [**35**], there are multiple ways to equally represent the OSC for a Euclidean space. Let $S = \{S_1, \ldots, S_m\}$ be an IFS on $\Delta \subset \mathbb{R}^d$, and A be the attractor of S. Define $A_i = S_i(A)$ to be the pre-fractals of A. Then $A_\sigma = S_{i_1} \circ S_{i_2} \circ \cdots \circ S_{i_k}(A)$ for each $\sigma \in D_k$. For the following, we say $\eta \in D_k$ is incomparable with $\tau \in D_m$, notated $\eta \not\sqsubset \tau$ if there does not exists σ such that $\eta \star \sigma = \tau$ or $\tau \star \sigma = \eta$. In this setting, the following are equivalent:

(1) (Due to Moran, [**29**]) An IFS $S = \{S_i\}_{i=1}^n$ is said to satisfy the OSC if there exists a non-empty open set U such that $S_i(U) \subseteq U$ for each i, and $S_i(U) \cap S_j(U) = \emptyset$ whenever $i \neq j$.
(2) (Due to Schief, [**36**]) Given $\varepsilon > 0$, there exists an integer N such that at most N incomparable pieces $\mathcal{A}_\sigma$ of diameter larger than or equal to ε can intersect the $\varepsilon-$neighborhood of a

piece $\mathcal{A}_\tau$ of diameter equal to ε. Two pieces of A, $\mathcal{A}_\sigma$ and $\mathcal{A}_\tau$, are said to be incomparable if $\sigma \not\sqsubseteq \tau$ and $\tau \not\sqsubseteq \sigma$.

(3) (Due to Moran and Shief, [**29**], [**36**]) $H^s(A) > 0$, where s is the unique solution to the equation $\sum_{i=1}^m c_i^s = 1$.

However, in some cases the open set U from the OSC may be disjoint from the attractor A of the IFS. Thus, there is a stronger version of the OSC that avoids this case.

Definition 2.7 ([**30**]). The Strong Open Set Condition (SOSC) holds if the set U in Definition 2.6 can be chosen with $U \cap A \neq \emptyset$, where A is the attractor of S.

In [**36**], Shief shows that for Euclidean space the OSC and SOSC are equivalent. The point of the OSC is to make sure the individual copies of the set made in the next generation do not overlap too much. For a more in-depth look at how separation conditions such as these affect the Hausdorff dimension in general metric spaces, see [**34**] and the references therein.

It turns out that if an IFS satisfies the OSC, then the Hausdorff dimension and the box dimension of the attractor is intimately related to the contraction coefficients of the maps themselves, and very easy to calculate.

Theorem 2.8 ([**12**]). *Let* $S = \{S_1, \ldots, S_m\}$ *be an IFS of similarities with contraction ratios* $\{c_i\}_{i=1}^n$ *and attractor* A. *If* S *satisfies the Open Set Condition, then* $\dim_H(A) = \dim_B(A) = s$ *where* s *is the unique real number such that*

$$\sum_{i=1}^m c_i^s = 1. \tag{2.2.9}$$

We call this number s *the similarity dimension of* A, *denoted* $s = \dim_s(A)$. *For this specific value of* s, *we also have* $0 < H^s(A) < \infty$.

The proof is important but technical (see [**12**]). Equation (2.2.9) is called the Moran (or Moran-Hutchinson) equation.

Example 2.2.1. Consider again the Cantor set $\mathcal{C}$. The two functions

$$S_1(x) = \frac{x}{3} \qquad \text{and} \qquad S_2(x) = \frac{x+2}{3} \tag{2.2.10}$$

where $S_i : [0,1] \to [0,1]$, define an IFS with attractor $\mathcal{C}$. See Figure 1.6. Notice that S_1 and S_2 each have a contraction coefficient of $1/3$, and that their images are disjoint. Thus the IFS $\{S_1, S_2\}$ satisfies the OSC with $U = (0,1)$, and the Hausdorff dimension of the Cantor set satisfies

$$\left(\frac{1}{3}\right)^s + \left(\frac{1}{3}\right)^s = 2 \cdot \left(\frac{1}{3}\right)^s = 1. \tag{2.2.11}$$

That is, $s = \dfrac{\ln 2}{\ln 3}$. Here, $H^s(\mathcal{C}) = 1$ (see [**12**] for calculation of the measure).

Example 2.2.2. Let Δ be the domain bounded by the equilateral triangle defined by connecting the three points $\begin{bmatrix} -1/2 & 1/2 & 0 \\ 0 & 0 & \sqrt{3}/2 \end{bmatrix}$ in $\mathbb{R}^2$. Define the following three similarities,

$$\begin{aligned} S_1(x,y) &= \left(\frac{x}{2} - \frac{1}{4}, \frac{y}{2}\right) \\ S_2(x,y) &= \left(\frac{x}{2} + \frac{1}{4}, \frac{y}{2}\right) \\ S_3(x,y) &= \left(\frac{x}{2}, \frac{y}{2} + \frac{\sqrt{3}}{4}\right). \end{aligned}$$

Then $S = \{S_1, S_2, S_3\}$ satisfies the OSC for U being the interior of Δ, and the Sierpinski triangle is the attractor of S. See Figure 1.7. Notice that the contraction coefficient for each function is $1/2$. Thus, the Hausdorff dimensions of the Sierpinski triangle is

$$\left(\frac{1}{2}\right)^s + \left(\frac{1}{2}\right)^s + \left(\frac{1}{2}\right)^s = 3 \cdot \left(\frac{1}{2}\right)^s = 1. \tag{2.2.12}$$

Thus, $s = \dfrac{\ln 3}{\ln 2}$. Here $H^s(A)$ is not actually known, and there is active research on the calculation of the measure of the Sierpinski triangle, see [**39**], [**20**].

In our next example we look at a fractal that does not match our intuition of how a set should look like when its dimension is an integer.

Example 2.2.3. Let $\Delta = [0,1]^2$. In this example, we create a fractal often called the Cantor Dust. Here we have that the Cantor Dust (see Figure 2.2) is the attractor of the following similarities:

$$
\begin{aligned}
S_1(x,y) &= \left(\frac{x}{4}, \frac{y}{4}+\frac{1}{2}\right)\\
S_2(x,y) &= \left(\frac{x}{4}+\frac{1}{4}, \frac{y}{4}\right)\\
S_3(x,y) &= \left(\frac{x}{4}+\frac{1}{2}, \frac{y}{4}+\frac{3}{4}\right)\\
S_4(x,y) &= \left(\frac{x}{4}+\frac{3}{4}, \frac{y}{4}+\frac{1}{4}\right).
\end{aligned}
$$

Since the contraction coefficients are $1/4$ and there are four maps, the Hausdorff dimension of the limit set satisfies $4(\frac{1}{4})^s = 1$. That is, the Hausdorff dimension of the attractor is 1. There are many versions of this fractal, as we can change the contraction ratios to be any number in $(0, 1/2)$. This fractal also has some curious properties with its projection in various directions. For a short discussion on this, see [**12**], Example 6.7.

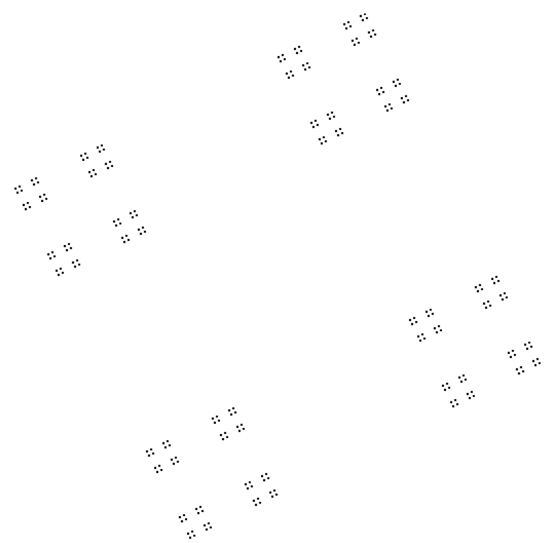

FIGURE 2.2. Attractor of $\{S_1, \ldots, S_4\}$

THEOREM 2.9 ([**14**]). *If a set F is self-similar, then*

$$\dim_H(F) = \underline{\dim}_B(F) = \overline{\dim}_B(F) = \dim_P(F) = \dim_{\mathcal{A}}(F) \leq \dim_s(F). \tag{2.2.13}$$

If we add in the property that F satisfies the OSC, then we get equality across the board.

THEOREM 2.10 ([**14**]). *If a set F is a self-similar set that satisfies the OSC, then*

$$\dim_H(F) = \underline{\dim}_B(F) = \overline{\dim}_B(F) = \dim_P(F) = \dim_{\mathcal{A}}(F) = \dim_s(F). \tag{2.2.14}$$

Using iterated function systems is a popular way to construct fractals, and has been used to great effect (e.g. [**2**], [**12**], [**19**]). For a survey of the current work in IFS theory, see [**6**] and the multitude of references therein.

We can see that the attractor of an IFS $\{S_1, S_2, \ldots, S_m\}$ is actually a special case of a Moran set. In MSC(2), define $n_k = m$ and set $S_\sigma = S_{i_k} \circ S_{i_{k-1}} \circ \cdots \circ S_{i_1}$ for $\sigma = (i_1, i_2, \cdots, i_k) \in D$. Then the resulting Moran set is self-similar and agrees with the attractor of the IFS. The dimension of the limit set can be quickly calculated from the Moran-Hutchinson formula in [**19**]. The fact that there is a formula (2.2.9) for computing the Hausdorff dimension of a large class of fractals created from IFSs is extremely convenient. A natural question arises: Can we construct more general fractals (e.g. non-self-similar Moran type sets) using an analogous approach while preserving the computational simplicity of the IFS? In the next chapter we present a method to do so.

CHAPTER 3

$\mathcal{F}-$Limit Sets

In this chapter, we extend ideas from IFS and Moran constructions in Chapter 2 by describing a new process that allows for the functions to be updated at every iteration while still maintaining the computational simplicity of an IFS. This process provides more variance in the limit sets (such as non-self-similarity) using an analogous approach to an IFS procedure. Estimates of the Hausdorff dimension of the limit sets created from such a process are given, and concrete examples are explored.

We first make the following observations about the general construction of a Moran set. Note that in the construction of a Moran set described in (2.1.4),

$$J_{\sigma*i} = S_i(J_\sigma), \text{ for all } i = 1, ...m, \text{ and } \sigma \in D. \tag{3.0.1}$$

Suppose that there is a tuning parameter in the expression of the function S_i (e.g. the coefficients a_i, b_i in a linear function $S_i(x) = a_i x + b_i$). One can tune the values of the parameter to get a comparable function. When J_σ is given, applying the comparable function to J_σ, as in equation (3.0.1), will not significantly change the computational complexity of constructing $J_{\sigma*i}$. The advantage of doing this at each iteration is that we introduce some variance into the limit set. Another observation is about which space the functions are defined. In classical IFS constructions, the functions are usually defined on all of the ambient space $\mathbb{R}^n$ (as in [**17**], the functions are $C^{1+\alpha}$ diffeomorphisms on $\mathbb{R}^n$). For our construction, we wish to relax the condition MSC(2) as well. Instead of restricting our attention to functions of higher regularity defined on the whole ambient space $\mathbb{R}^n$, we use maps from a collection of subsets to itself.

We will proceed as follows. In Section 3.1 we find bounds for the Hausdorff dimension of the limit sets in a general metric space setting of a collection of bounded sets, not necessarily satisfying the MSC conditions. Then in Section 3.2 we formulate the general setup for the construction of

Moran-type limit sets using the ideas from a modified IFS procedure, as discussed in the previous paragraph. In our construction we relax MSC(2) so that the limit set is not necessarily self-similar. More importantly, we drop MSC(4) from the construction process so that there are no limitations on the ratios of the diameters of the sets. Specifically, the ratio $\dfrac{diam(J_{\sigma*j})}{diam(J_\sigma)}$ in (2.1.6) is not limited to depend on just k and j, but varies with σ. This change allows us to produce a mosaic of possible fractals. An important observation is that the computational complexity of generating these fractals is the same as using an analogous, standard IFS. In Section 3.3 we give estimates of the Hausdorff dimension of the limit sets created from the general construction. In Section 3.4 we apply the results to specific examples, including modifications of the Cantor set, the Sierpinski triangle, and the Menger sponge.

3.1. Hausdorff Dimension of the Limit Sets

In this section we investigate the Hausdorff dimension $\dim_H(F)$ of the fractals F defined in (2.1.4), which do not necessarily satisfy all the MSC conditions. To start, we determine an upper bound for the dimension of the limit set F by considering the step-wise relative ratios between the diameters of sets.

Proposition 3.1. *Suppose $\mathcal{J} := \{J_\sigma : \sigma \in D\}$ is a collection of bounded subsets of a metric space (X, d), and $s > 0$. Let $E_k = \bigcup_{\sigma\in D_k} J_\sigma$, and $F = \bigcap_{k\geq 0} E_k$ be defined as in (2.1.4). If there exists a sequence of positive numbers $\{c_k\}_{k=1}^{\infty}$ such that*

$$\liminf_{k\to\infty} \prod_{i=1}^{k} c_i = 0$$

and

$$\sum_{j=1}^{n_k} (\mathrm{diam}(J_{\sigma*j}))^s \leq c_k\, (\mathrm{diam}(J_\sigma))^s\,, \tag{3.1.1}$$

for all $\sigma \in D_{k-1}$ and all $k = 1, 2, \cdots$, then $dim_H(F) \leq s$.

Proof. We prove by using mathematical induction that for $k = 1, 2, \cdots$,

$$\sum_{\sigma\in D_k} (\mathrm{diam}(J_\sigma))^s \leq \left(\prod_{i=1}^{k} c_i\right) (diam(J_\emptyset))^s. \tag{3.1.2}$$

When $k = 1$, (3.1.2) follows from (3.1.1). Now assume (3.1.2) is true for some $k \geq 1$. Then by (2.1.3), (3.1.1), and (3.1.2),

$$\begin{aligned}
\sum_{\sigma \in D_{k+1}} (\mathrm{diam}(J_\sigma))^s &= \sum_{\sigma \in D_k} \left(\sum_{j=1}^{n_{k+1}} (\mathrm{diam}(J_{\sigma * j}))^s \right) \\
&\leq c_{k+1} \sum_{\sigma \in D_k} (\mathrm{diam}(J_\sigma))^s \\
&\leq \left(\prod_{i=1}^{k+1} c_i \right) (\mathrm{diam}(J_\emptyset))^s
\end{aligned}$$

as desired. By the induction principle, (3.1.2) holds for all $k = 1, 2, \cdots$.

For each k, set

$$\delta_k = \max\{\mathrm{diam}(J_\sigma) : \sigma \in D_k\} > 0.$$

Then, by (3.1.2), $\delta_k \leq \left(\prod_{i=1}^k c_i\right)^{1/s} \mathrm{diam}(J_\emptyset)$. Moreover, by (3.1.2)

$$\mathcal{H}^s_{\delta_k}(F) \leq \mathcal{H}^s_{\delta_k}(E_k) \leq \sum_{\sigma \in D_k} \alpha(s) \left(\frac{\mathrm{diam}(J_\sigma)}{2} \right)^s \leq \left(\prod_{i=1}^k c_i \right) \alpha(s) \left(\frac{\mathrm{diam}(J_\emptyset)}{2} \right)^s.$$

Since $\liminf_{k\to\infty} \prod_{i=1}^k c_i = 0$, there exists a sequence $\{k_t\}_{t=1}^\infty$ such that

$$\lim_{t\to\infty} \prod_{i=1}^{k_t} c_i = 0. \tag{3.1.3}$$

Thus, $\delta_{k_t} \to 0$ as $t \to \infty$, and $\mathcal{H}^s(F) = \lim_{t\to\infty} \mathcal{H}^s_{\delta_{k_t}}(F) = 0$, and hence $\dim_H(F) \leq s$. □

Conversely, a lower bound on the Hausdorff dimension of the limit set F can also be obtained as follows.

Definition 3.2. Let $\mathcal{J} := \{J_\sigma : \sigma \in D\}$ be a collection of compact subsets of a metric space (X, d), and F be the limit set of $\mathcal{J}$ as given in (2.1.4). $\mathcal{J}$ is said to satisfy the *uniform covering condition* if there exists a real number $\gamma > 0$ and a natural number N such that for all closed ball B in X, there exists a subset $D_B \subset D$ with cardinality of D_B at most N,

$$B \cap F \subseteq \bigcup_{\sigma \in D_B} J_\sigma \text{ and } diam(B) \geq \gamma \sum_{\sigma \in D_B} diam(J_\sigma). \tag{3.1.4}$$

Proposition 3.3. *Let $\mathcal{J} := \{J_\sigma : \sigma \in D\}$ be a collection of compact subsets of a metric space (X, d) with diam$(J_\emptyset) > 0$, and F be the limit set of $\mathcal{J}$ as given in (2.1.4). If $\mathcal{J}$ satisfies the uniform covering condition, and if for some $s > 0$,*

$$\sum_{j=1}^{n_k} \operatorname{diam}(J_{\sigma*j})^s \geq \operatorname{diam}(J_\sigma)^s \tag{3.1.5}$$

for all $\sigma \in D_{k-1}$ and all $k = 1, 2, \cdots$, then $dim_H(F) \geq s$.

Proof. We first show that under condition (3.1.5), there exists a probability measure μ on X concentrated on F such that for each $\sigma \in D$,

$$\mu(J_\sigma) \leq \left(\frac{\operatorname{diam}(J_\sigma)}{\operatorname{diam}(J_\emptyset)} \right)^s . \tag{3.1.6}$$

Let $\mu(J_\emptyset) = 1$, and for each $\sigma \in D_k$ for $k > 0$ and $i = 1, \cdots, n_k$, we inductively set

$$\mu(J_{\sigma*i}) = \frac{\operatorname{diam}(J_{\sigma*i})^s}{\sum_{j=1}^{n_k} \operatorname{diam}(J_{\sigma*j})^s} \mu(J_\sigma).$$

For any Borel set A in X, define

$$\mu(A) = \inf \left\{ \sum_{i=1}^{\infty} \mu(J_{\sigma_i}) : A \cap F \subset \bigcup_{i=1}^{\infty} J_{\sigma_i} \text{ and } J_{\sigma_i} \in \mathcal{J} \right\}.$$

One can check that μ defines a probability measure on X, concentrated on F.

To prove (3.1.6) for J_σ, $\forall \sigma \in D$, we proceed by using induction on k when $\sigma \in D_k$. It is clear for $k = 0$. Now assume that (3.1.6) holds for each $\sigma \in D_k$ for some k. Then by induction assumption and (3.1.5), for each $i = 1, \cdots, n_{k+1}$,

$$\begin{aligned}
\mu(J_{\sigma*i}) &= \frac{\operatorname{diam}(J_{\sigma*i})^s}{\sum_{j=1}^{n_k} \operatorname{diam}(J_{\sigma*j})^s} \mu(J_\sigma) \\
&\leq \frac{\operatorname{diam}(J_{\sigma*i})^s}{\sum_{j=1}^{n_k} \operatorname{diam}(J_{\sigma*j})^s} \left(\frac{\operatorname{diam}(J_\sigma)}{\operatorname{diam}(J_\emptyset)} \right)^s \\
&\leq \left(\frac{\operatorname{diam}(J_{\sigma*i})}{\operatorname{diam}(J_\emptyset)} \right)^s .
\end{aligned}$$

This proves inequality (3.1.6).

Now, for any $\delta > 0$, let $\{B_i\}$ be any collection of closed balls with $\text{diam}(B_i) \leq \delta$ and $F \subseteq \cup_i B_i$. For each i, let D_{B_i} be the subset of D corresponding to B_i as given in equation (3.1.4). Note that

$$F \subseteq \bigcup_i B_i \cap F \subseteq \bigcup_i \bigcup_{\sigma \in D_{B_i}} J_\sigma = \bigcup_{\sigma \in \tilde{D}} J_\sigma,$$

where $\tilde{D} := \cup_{i=1}^{\infty} D_{B_i} \subseteq D$.

Let

$$\begin{aligned} C(s) &:= \max\{\sum_{i=1}^{N} (x_i)^s : (x_1, x_2, \cdots, x_N) \in [0,1]^N \text{ with } \sum_{i=1}^{N} x_i = 1\} \\ &= \begin{cases} N^{1-s}, & \text{if } 0 < s < 1 \\ 1, & \text{if } s \geq 1. \end{cases} \end{aligned}$$

and $c(s) = \frac{\alpha(s)}{C(s)} \left(\frac{\gamma \text{diam}(J_\emptyset)}{2} \right)^s > 0$. Then, by (3.1.4) and (3.1.6),

$$\begin{aligned} & \sum_i \alpha(s) \left(\frac{\text{diam}(B_i)}{2} \right)^s \\ \geq \ & \sum_i \frac{\alpha(s)}{2^s} \left(\gamma \sum_{\sigma \in D_{B_i}} \text{diam}(J_\sigma) \right)^s \\ \geq \ & \sum_i \frac{\alpha(s)}{2^s C(s)} \gamma^s \sum_{\sigma \in D_{B_i}} (\text{diam}(J_\sigma))^s \\ \geq \ & \frac{\alpha(s)}{2^s C(s)} \gamma^s \sum_{\sigma \in \tilde{D}} (\text{diam}(J_\sigma))^s \\ \geq \ & \frac{\alpha(s)}{2^s C(s)} \gamma^s \, (\text{diam}(J_\emptyset))^s \sum_{\sigma \in \tilde{D}} \mu(J_\sigma) \\ \geq \ & c(s) \mu \left(\sum_{\sigma \in \tilde{D}} J_\sigma \right) \geq c(s) \mu(F) = c(s). \end{aligned}$$

Thus, $\mathcal{H}^s(F) = \lim_{\delta \to 0} \mathcal{H}^s_\delta(F) \geq c(s) > 0$, and hence $\dim_H(F) \geq s$. $\square$

In section 3.5 we will explore sufficient conditions for $\mathcal{J}$ to satisfy the uniform covering condition.

3.2. General Setup of $\mathcal{F}$-Limit sets

We now formalize the ideas from Chapter 2 and Section 3.1 to give a description of the construction of such generalized fractals. We concentrate on the maps in order to take advantage of the computational nature of an IFS, but allow for the maps to be updated and changed at each iteration.

In this section, let $\mathcal{X}$ be a collection of nonempty compact subsets of a metric space.

DEFINITION 3.4. A mapping $f : \mathcal{X} \to \mathcal{X}$ is called a *compression* on $\mathcal{X}$ if $f(E) \subseteq E$ for each $E \in \mathcal{X}$.

For each natural number m, let

$$\mathcal{C}_m(\mathcal{X}) = \{(f^{(1)}, f^{(2)}, \ldots, f^{(m)}) : f_i \text{ is a compression on } \mathcal{X}, i = 1, \ldots, m\}.$$

DEFINITION 3.5. Let $\mathcal{M}$ be a nonempty set. A mapping

$$\mathcal{F}: \quad \mathcal{M} \to \mathcal{C}_m(\mathcal{X}) \tag{3.2.1}$$

$$k \to f_k = (f_k^{(1)}, f_k^{(2)}, \cdots, f_k^{(m)}). \tag{3.2.2}$$

is called a marking of $\mathcal{C}_m(\mathcal{X})$ by $\mathcal{M}$. Each element $k \in \mathcal{M}$ is called the marker of f_k.

Given a marking $\mathcal{F}$ and an initial set $E_0 \in \mathcal{X}$, we will construct a generalized Moran set from any sequence of markers in $\mathcal{M}$. Note that any sequence $\{k_\ell\}_{\ell=0}^{\infty}$ in $\mathcal{M}$ can be represented as a mapping from the ordered set D to $\mathcal{M}$.

DEFINITION 3.6. Let $\mathcal{F}$ be a marking of $\mathcal{C}_m(\mathcal{X})$ by $\mathcal{M}$, let E_0 be any element in $\mathcal{X}$, and D be as in (2.1.1). Suppose $\vec{k} : D \to \mathcal{M}$ is a map sending σ to k_σ. For each $\sigma \in D$ and $1 \leq j \leq m$, we recursively define $J_\emptyset = E_0$ and

$$J_{\sigma * j} = f_{\mathbf{k}_\sigma}^{(j)}(J_\sigma), \tag{3.2.3}$$

where f_{k_σ} is given by $\mathcal{F}$ as in (3.2.2).

The limit set $F = \bigcap_{k \geq 1} \bigcup_{\sigma \in D_k} J_\sigma$ associated with $\mathcal{J}(\vec{k}) = \{J_\sigma : \sigma \in D\}$ is called the $\mathcal{F}$-limit set generated by $\vec{k}$ with the initial set E_0.

We now make two observations relating the concepts of an $\mathcal{F}$-limit set with the attractor of an IFS.

We first observe that the attractor of an IFS $\{S_1, S_2, \ldots, S_m\}$ on a closed subset Δ of $\mathbb{R}^n$ can be viewed as an $\mathcal{F}$-limit set as follows.

Let $\mathcal{X} = \{E : E \text{ is a non-empty compact subset of } \Delta, S_i(E) \subseteq E, \text{ for all } i\}$. Since each S_i is a contraction on Δ, the set $E_r := \Delta \cap \overline{B(0,r)}$ is a non-empty compact subset of Δ, and $S_i(E_r) \subseteq E_r$ for each i when r is sufficiently large. In other words, $E_r \in \mathcal{X}$ for sufficiently large r. Also, each contraction map S_i acting on Δ naturally determines a map $f^{(i)} : \mathcal{X} \to \mathcal{X}$ given by

$$f^{(i)}(E) = S_i(E) := \{S_i(x) \mid x \in E \subseteq \Delta\} \tag{3.2.4}$$

for each $E \in \mathcal{X}$. Since $f^{(i)}(E) = S_i(E) \subseteq E$, $f^{(i)}$ is a compression for each i. Set

$$f = (f^{(1)}, f^{(2)}, \ldots, f^{(m)}).$$

For any non-empty set $\mathcal{M}$, define the marking $\mathcal{F}$ of $\mathcal{C}_m(\mathcal{X})$ to be the constant function $\mathcal{F}(k) = f$ for all $k \in \mathcal{M}$. Thus, for each $\sigma \in D_k$ and $i = 1, \ldots, m$, we have that $J_{\sigma * i} = S_i(J_\sigma)$ from (3.2.3). As a result, for any map $\vec{k} : D \to \mathcal{M}$, the collection $\mathcal{J}(\vec{k}) = \{J_\sigma : \sigma \in D\}$ is independent of the choice of $\vec{k}$. Thus, the associated $\mathcal{F}$-limit set $F = \bigcap_{k \geq 1} \bigcup_{\sigma \in D_k} J_\sigma$ agrees with the attractor of the given IFS $\{S_1, S_2, \ldots, S_m\}$.

Conversely, let $\mathcal{F}$ be a marking of $\mathcal{C}_m(\mathcal{X})$ by $\mathcal{M}$ where $\mathcal{X}$ is a collection of non-empty compact subsets of Δ. Suppose there is a mapping $\vec{k} : D \to \mathcal{M}$ such that the sequence $\{f_{k_\sigma}\}_{\sigma \in D}$ is constant in $\mathcal{C}_m(\mathcal{X})$ (i.e. there exists an $f \in \mathcal{C}_m(\mathcal{X})$ such that $f_{k_\sigma} = f$ for all $\sigma \in D$) and for each $i = 1, 2, \ldots, m$, there exists a contraction S_i on Δ such that equation (3.2.4) holds for each $E \in \mathcal{X}$. Then the $\mathcal{F}$-limit set F generated by $\vec{k}$ is the attractor of the IFS $\{S_1, S_2, \ldots, S_m\}$.

Therefore, choosing $\vec{k} : D \to \mathcal{M}$ to be a constant map will result in a limit set F that is the attractor of an IFS. In the above sense, our approach is a generalization of the standard IFS construction.

An important observation is that replacing $\{k_\sigma\}_{\sigma \in D}$ by another sequence $\{\tilde{k}_\sigma\}_{\sigma \in D}$ in (3.2.3) will not change the computational complexity of the construction of $\mathcal{J}(\vec{k})$. Thus, generating the limit set F will have a similar computational complexity as generating the attractor of a comparable IFS.

In the following section we will compute the Hausdorff dimension of the constructed $\mathcal{F}$-limit sets. In section 5 we will provide examples along with their dimensions.

3.3. Hausdorff dimensions of $\mathcal{F}$-Limit sets

As indicated in Propositions 3.1 and 3.3, the relative ratio between the diameters of the sets plays an important role in the calculation of the dimension of the limit set. Therefore, we introduce the following definition.

Definition 3.7. For any compression $g : \mathcal{X} \to \mathcal{X}$, define

$$U(g) = \sup_{E \in \mathcal{X}} \frac{\operatorname{diam}(g(E))}{\operatorname{diam}(E)}, \text{ and } L(g) = \inf_{E \in \mathcal{X}} \frac{\operatorname{diam}(g(E))}{\operatorname{diam}(E)}. \tag{3.3.1}$$

Note that, for each $E \in \mathcal{X}$,

$$L(g) \cdot \operatorname{diam}(E) \leq \operatorname{diam}(g(E)) \leq U(g) \cdot \operatorname{diam}(E). \tag{3.3.2}$$

For any $\mathbf{k} \in \mathcal{M}$ and $f_{\mathbf{k}} = (f_{\mathbf{k}}^{(1)}, f_{\mathbf{k}}^{(2)}, \cdots, f_{\mathbf{k}}^{(m)}) \in \mathcal{C}_m(\mathcal{X})$, define

$$\mathbf{U}_{\mathbf{k}} = \left(U(f_{\mathbf{k}}^{(1)}), \cdots, U(f_{\mathbf{k}}^{(m)})\right) \in \mathbb{R}^m,$$

and

$$\mathbf{L}_{\mathbf{k}} = \left(L(f_{\mathbf{k}}^{(1)}), \cdots, L(f_{\mathbf{k}}^{(m)})\right) \in \mathbb{R}^m.$$

Also, for each $x = (x_1, \cdots, x_m) \in \mathbb{R}^m$ and $s > 0$, denote

$$||x||_s = \left(\sum_{i=1}^{m} |x_i|^s\right)^{\frac{1}{s}}.$$

These notations, Proposition 3.1 and Proposition 3.3 motivate our main theorem.

Theorem 3.8. *Let F be the $\mathcal{F}$-limit set generated by a sequence $\{\mathbf{k}_\sigma\}_{\sigma \in D}$ with initial set $J_\emptyset$, and $s > 0$.*

(a) *If F satisfies the uniform covering condition (3.1.4) and*

$$\inf_{\sigma\in D}\{||\mathbf{L}_{\mathbf{k}_\sigma}||_s\} \geq 1,$$

then $\dim_H(F) \geq s$.

(b) *If*

$$\sup_{\sigma\in D}\{||\mathbf{U}_{\mathbf{k}_\sigma}||_s\} < 1,$$

then $\dim_H(F) \leq s$.

PROOF. (a) By (3.2.3) and (3.3.2), for all $\sigma \in D$,

$$\sum_{j=1}^{m} \mathrm{diam}(J_{\sigma*j})^s = \sum_{j=1}^{m} \mathrm{diam}\left(f^{(j)}_{\mathbf{k}_\sigma}(J_\sigma)\right)^s \geq \sum_{j=1}^{m}\left(L(f^{(j)}_{\mathbf{k}_\sigma})\right)^s \mathrm{diam}(J_\sigma)^s \geq \mathrm{diam}(J_\sigma)^s.$$

Thus, by Proposition 3.3, $\dim_H(F) \geq s$.

(b) Similarly, for all $\sigma \in D$,

$$\sum_{j=1}^{m} \mathrm{diam}(J_{\sigma*j})^s \leq \sum_{j=1}^{m}\left(U(f^{(j)}_{\mathbf{k}_\sigma})\right)^s \mathrm{diam}(J_\sigma)^s \leq c\cdot \mathrm{diam}(J_\sigma)^s,$$

where

$$c := \sup_{\sigma}\{(||\mathbf{U}_{\mathbf{k}_\sigma}||_s)^s\} < 1.$$

By Proposition 3.1, $\dim_H(F) \leq s$. □

REMARK 3.9. For practical reasons, we find that it is more convenient to represent the mapping $\vec{k} : D \to \mathcal{M}$ by a sequence $\{k_\ell\}_{\ell=0}^{\infty} \subseteq \mathcal{M}$. For each $\sigma = (i_1, i_2, \ldots, i_k) \in D_k$, let

$$\ell(\sigma) = \sum_{p=0}^{k-1} m^p i_{k-p} \tag{3.3.3}$$

be the ordering of σ in the ordered set D. Using this notation, we can rewrite Definition 3.6 as follows.

Definition 3.6'. Let $\mathcal{F}$ be a marking of $\mathcal{C}_m(\mathcal{X})$ by $\mathcal{M}$, let $\{\mathbf{k}_\ell\}_{\ell=0}^{\infty}$ be a sequence in $\mathcal{M}$, and $E_0 \in \mathcal{X}$ be a starting set. For each $\ell = 0, 1, 2, \cdots$ and $j = 1, 2, \cdots, m$, we iteratively denote the set

$$E_{m\ell+j} = f^{(j)}_{\mathbf{k}_\ell}(E_\ell) \in \mathcal{X},$$

where $f_{\mathbf{k}_\ell}$ is given by $\mathcal{F}$ as in (3.2.2).

Let $\mathcal{G}_m(0) = 0$ and for $n \geq 1$,

$$\mathcal{G}_m(n) = m + m^2 + \cdots + m^n = \frac{m^{n+1} - m}{m - 1} \tag{3.3.4}$$

denote the number of sets in the n^{th} generation, i.e. the cardinality of D_n.

The limit set

$$F = \bigcap_{n=1}^{\infty} \bigcup_{\ell=\mathcal{G}_m(n-1)+1}^{\mathcal{G}_m(n)} E_\ell \tag{3.3.5}$$

is called the $\mathcal{F}$-limit set generated by the triple $(\mathcal{F}, \{\mathbf{k}_\ell\}_{\ell=0}^{\infty}, E_0)$.

In the following, we will use the notation from Definition 3.6' to describe the construction of the $\mathcal{F}$-limit sets. Clearly, using this notation, Theorem 3.8 simply says that if F satisfies the uniform covering condition (3.1.4) and $\inf_\ell\{||\mathbf{L}_{\mathbf{k}_\ell}||_s\} \geq 1$, then $\dim_H(F) \geq s$, and if $\sup_\ell\{||\mathbf{U}_{\mathbf{k}_\ell}||_s\} < 1$, then $\dim_H(F) \leq s$.

When both $\{||\mathbf{L}_{\mathbf{k}_\ell}||_s\}_{\ell=0}^{\infty}$ and $\{||\mathbf{U}_{\mathbf{k}_\ell}||_s\}_{\ell=0}^{\infty}$ are convergent sequences, the following corollary enables us to quickly estimate the dimension of F.

COROLLARY 3.10. *Let F be the limit set generated by the triple $(\mathcal{F}, \{\mathbf{k}_\ell\}_{\ell=0}^{\infty}, E_0)$.*

(a) *Let* $\underline{s_*} := \sup\{s : \liminf_{\ell\to\infty}\{||\mathbf{L}_{\mathbf{k}_\ell}||_s\} > 1\}$. *Then*

$$\dim_H(F) \geq \underline{s_*}, \tag{3.3.6}$$

provided F satisfies the uniform covering condition (3.1.4).

(b) *Let* $\overline{s^*} := \inf\{s : \limsup_{\ell\to\infty}\{||\mathbf{U}_{\mathbf{k}_\ell}||_s\} < 1\}$. *Then*

$$\dim_H(F) \leq \overline{s^*}. \tag{3.3.7}$$

PROOF. For any $0 < s < \underline{s_*}$, by the definition of $\underline{s_*}$,

$$\liminf_{\ell\to\infty}\{||\mathbf{L}_{\mathbf{k}_\ell}||_s\} > 1.$$

Thus, when $\ell_* \in \mathbb{N}$ is large enough,

$$\inf_{\ell \geq \ell_*} \{||\mathbf{L}_{\mathbf{k}_\ell}||_s\} \geq 1, \qquad \text{i.e. } \inf_{\ell \geq 0} \{||\mathbf{L}_{\mathbf{k}_{\ell_*+\ell}}||_s\} \geq 1.$$

Since $F \cap E_{\ell_*}$ is the set generated by the triple $(\mathcal{F}, \{\mathbf{k}_{\ell_*+\ell}\}_{\ell=0}^{\infty}, E_{\ell_*})$, by Theorem 3.8, it follows that $\dim_H(F \cap E_{\ell_*}) \geq s$ for any ℓ_* large enough. This implies that $\dim_H(F) \geq s$ for any $s < \underline{s_*}$ and hence $\dim_H(F) \geq \underline{s_*}$.

Similarly, we also have $\dim_H(F) \leq \overline{s^*}$. □

In the following corollaries, we will see that bounds of the dimension of F can also be obtained from corresponding bounds on $\mathbf{L}_{\mathbf{k}_\ell}$ and $\mathbf{U}_{\mathbf{k}_\ell}$.

Notation. For any two points $x = (x_1, \cdots, x_m)$ and $y = (y_1, \cdots, y_m)$ in $\mathbb{R}^m$, we say $x \leq y$ if $x_i \leq y_i$ for each $i = 1, \cdots, m$.

Corollary 3.11. *Let $\mathbf{t} = (t_1, \cdots, t_m)$ and $\mathbf{r} = (r_1, \cdots, r_m)$ be two points in $(0,1)^m \subset \mathbb{R}^m$. Let s_* and s^* be the solutions to $||\mathbf{t}||_{s_*} = 1$, and $||\mathbf{r}||_{s^*} = 1$ respectively, i.e.*

$$t_1^{s_*} + t_2^{s_*} + \cdots + t_m^{s_*} = 1, \text{ and } r_1^{s^*} + r_2^{s^*} + \cdots + r_m^{s^*} = 1.$$

(a) *If $\mathbf{L}_{\mathbf{k}_\ell} \geq \mathbf{t}$ for all ℓ and F satisfies the uniform covering condition (3.1.4), then $\dim_H(F) \geq s_*$.*

(b) *If $\mathbf{U}_{\mathbf{k}_\ell} \leq \mathbf{r}$ for all ℓ, then $\dim_H(F) \leq s^*$.*

(c) *If $\mathbf{L}_{\mathbf{k}_\ell} = \mathbf{r} = \mathbf{U}_{\mathbf{k}_\ell}$ for all ℓ and F satisfies the uniform covering condition (3.1.4), then $\dim_H(F) = s^*$.*

Proof. (a) Let $0 < s < s_*$. Then,

$$\inf_{\ell} \{||\mathbf{L}_{\mathbf{k}_\ell}||_s\} \geq ||\mathbf{t}||_s \geq ||\mathbf{t}||_{s_*} = 1.$$

Thus, by Theorem 3.8, $\dim_H(F) \geq s$ for any $s < s_*$, and hence $\dim_H(F) \geq s_*$.

(b) Similarly, let $0 < s^* < s$. Then,

$$\sup_{\ell} \{||\mathbf{U}_{\mathbf{k}_\ell}||_s\} \leq ||\mathbf{r}||_s < ||\mathbf{r}||_{s^*} = 1.$$

Thus, by Theorem 3.8, $\dim_H(F) \leq s$ for any $s > s^*$, and hence $\dim_H(F) \leq s^*$.

(c) follows from (a) and (b). $\square$

A special case of Corollary 3.11 gives the following explicit formulas for the bounds on the dimension of F.

COROLLARY 3.12. *Let F be the limit set generated by the triple $(\mathcal{F}, \{\mathbf{k}_\ell\}_{\ell=0}^{\infty}, E_0)$. Let*

$$\mathbf{t} = (t, \cdots, t) \text{ and } \mathbf{r} = (r, \cdots, r),$$

for some $0 < t, r < 1$.

(a) *If $\mathbf{L}_{\mathbf{k}_\ell} \geq \mathbf{t}$ for all ℓ and F satisfies the uniform covering condition (3.1.4), then $\dim_H(F) \geq \frac{\log m}{-\log t}$.*
(b) *If $\mathbf{U}_{\mathbf{k}_\ell} \leq \mathbf{r}$ for all ℓ, then $\dim_H(F) \leq \frac{\log m}{-\log r}$.*
(c) *If $\mathbf{L}_{\mathbf{k}_\ell} = \mathbf{r} = \mathbf{U}_{\mathbf{k}_\ell}$ for all ℓ and F satisfies the uniform covering condition (3.1.4), then $\dim_H(F) = \frac{\log m}{-\log r}$.*

Other types of bounds on $\mathbf{L}_{\mathbf{k}_\ell}$ and $\mathbf{U}_{\mathbf{k}_\ell}$ can also be used to provide bounds on $\dim_H(F)$, as indicated by the following result.

COROLLARY 3.13. *Let F be the limit set generated by the triple $(\mathcal{F}, \{\mathbf{k}_\ell\}_{\ell=0}^{\infty}, E_0)$.*

(a) *If F satisfies the uniform covering condition (3.1.4) and*

$$w := \inf_{\ell}\{||\mathbf{L}_{\mathbf{k}_\ell}||_1\} \geq 1,$$

then $\dim_H(F) \geq \frac{\log(m)}{\log(m)-\log(w)}$.

(b) *If*

$$u := \sup_{\ell}\{||\mathbf{U}_{\mathbf{k}_\ell}||_1\} < 1,$$

then $\dim_H(F) \leq \frac{\log(m)}{\log(m)-\log(u)}$.

PROOF. (a). In this case, for $s = \frac{\log(m)}{\log(m)-\log(w)} \geq 1$, we have

$$\frac{\sum_{j=1}^{m}\left(L\left(f_{\mathbf{k}_\ell}^{(j)}\right)\right)^s}{m} \geq \left(\frac{\sum_{j=1}^{m} L\left(f_{\mathbf{k}_\ell}^{(j)}\right)}{m}\right)^s \geq \left(\frac{w}{m}\right)^s$$

for each ℓ. Thus,

$$\inf_{\ell}\{||\mathbf{L}_{\mathbf{k}_\ell}||_s\} \geq m^{\frac{1}{s}}\frac{w}{m} = 1,$$

then by Theorem 3.8, $\dim_H(F) \geq s$.

(b). In this case, for any $1 \geq s > \frac{\log(m)}{\log(m)-\log(u)}$, we have

$$\frac{\sum_{j=1}^{m}\left(U\left(f_{\mathbf{k}_\ell}^{(j)}\right)\right)^s}{m} \leq \left(\frac{\sum_{j=1}^{m}U\left(f_{\mathbf{k}_\ell}^{(j)}\right)}{m}\right)^s \leq \left(\frac{u}{m}\right)^s$$

for each ℓ. Thus,

$$\sup_{\ell}\{||\mathbf{U}_{\mathbf{k}_\ell}||_s\} \leq m^{\frac{1}{s}}\frac{u}{m} < 1.$$

By Theorem 3.8, $\dim_H(F) \leq s$. Hence, $\dim_H(F) \leq \frac{\log(m)}{\log(m)-\log(u)}$. $\square$

Note that this corollary generally provides better bounds on $\dim_H(F)$ than those obtained from directly applying Theorem 3.8.

3.4. Examples of $\mathcal{F}$-Limit sets

In this section we describe the construction of both classical fractals and generalized Moran sets in the language of Section 3.2, and calculate the dimension using the results from Section 3.3.

3.4.1. Cantor-Like Sets. We first consider Cantor-like sets. Let

$$\mathcal{X} = \{[a,b] : a, b \in \mathbb{R}\} \tag{3.4.1}$$

be the collection of closed intervals, $m = 2$, and let $\mathcal{M} = [0,1]^2 \subseteq \mathbb{R}$. For each $\mathbf{k} = (k^{(1)}, k^{(2)}) \in \mathcal{M}$, we consider the following two maps,

$$\begin{aligned} f_{\mathbf{k}}^{(1)} : \quad \mathcal{X} &\to \mathcal{X} \\ [a,b] &\mapsto [a, k^{(1)}(b-a)+a] \end{aligned}$$

$$\begin{aligned} f_{\mathbf{k}}^{(2)} : \quad \mathcal{X} &\to \mathcal{X} \\ [a,b] &\mapsto [k^{(2)}(a-b)+b, b]. \end{aligned}$$

Note that both $f_{\mathbf{k}}^{(1)}$ and $f_{\mathbf{k}}^{(2)}$ are compression maps for any $\mathbf{k} \in \mathcal{M}$. Thus, this defines a marking

$$\begin{aligned} \mathcal{F}: \quad \mathcal{M} &\to \mathcal{C}_2(\mathcal{X}) \\ \mathbf{k} &\mapsto f_{\mathbf{k}} = (f_{\mathbf{k}}^{(1)}, f_{\mathbf{k}}^{(2)}). \end{aligned}$$

Here, for each $\mathbf{k} = (k^{(1)}, k^{(2)}) \in \mathcal{M}$, one can clearly see that

$$\operatorname{diam}\left(f_{\mathbf{k}}^{(i)}([a,b])\right) = k^{(i)} \cdot \operatorname{diam}([a,b]).$$

Thus, $L\left(f_{\mathbf{k}}^{(i)}\right) = k^{(i)} = U\left(f_{\mathbf{k}}^{(i)}\right)$, and hence

$$\mathbf{L}_{\mathbf{k}} = \mathbf{k} = \mathbf{U}_{\mathbf{k}}. \tag{3.4.2}$$

Let $E_0 = [0,1] \in \mathcal{X}$ be fixed. For any sequence $\{\mathbf{k}_\ell\}_{\ell=0}^{\infty} \in \mathcal{M}$, we define the following:

$$\begin{aligned}
E^{(0)} &= E_0 \\
E^{(1)} &= f_{\mathbf{k}_0}^{(1)}(E_0) \cup f_{\mathbf{k}_0}^{(2)}(E_0) =: E_1 \cup E_2 \\
E^{(2)} &= f_{\mathbf{k}_1}^{(1)}(E_1) \cup f_{\mathbf{k}_1}^{(2)}(E_1) \cup f_{\mathbf{k}_2}^{(1)}(E_2) \cup f_{\mathbf{k}_2}^{(2)}(E_2) \\
&:= \quad E_3 \quad \cup \quad E_4 \quad \cup \quad E_5 \quad \cup \quad E_6 \\
&\vdots \\
E^{(n)} &= \bigcup_{i=2^{n-1}-1}^{2^n-2} \left(f_{\mathbf{k}_i}^{(1)}(E_i) \cup f_{\mathbf{k}_i}^{(2)}(E_i)\right) := \bigcup_{i=2^{n-1}-1}^{2^n-2} (E_{2i+1} \cup E_{2i+2}) = \bigcup_{\ell=2^n-1}^{2(2^n-1)} E_\ell.
\end{aligned}$$

Note that when $\mathbf{k}_\ell = (\frac{1}{3}, \frac{1}{3})$ for all ℓ, $E^{(n)}$ is the n^{th}-generation of the Cantor set $\mathcal{C}$ and $F = \lim_{n\to\infty} E^{(n)} = \bigcap_n E^{(n)} = \mathcal{C}$.

Observe that the process of constructing the sequence $\{E^{(n)}\}_{n=0}^{\infty}$ is independent of the values of $\{\mathbf{k}_\ell\}_{\ell=0}^{\infty}$. To allow for more general outcomes, we can update the linear functions $f_{\mathbf{k}}^{(1)}$ and $f_{\mathbf{k}}^{(2)}$ simply by changing the value of $\mathbf{k}$ at each stage of the construction, which does not change the computational complexity of the process. Using this idea, we now construct some examples of Cantor-like sets by choosing suitable sequences $\{\mathbf{k}_\ell\}_{\ell=0}^{\infty}$.

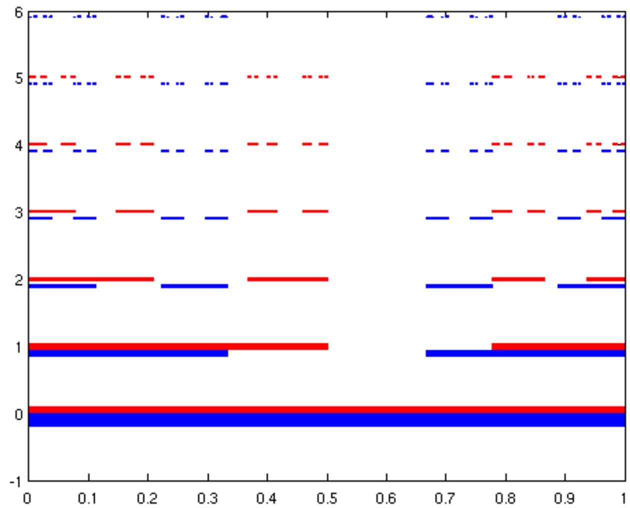

FIGURE 3.1. Comparison of classical Cantor set (blue) and new Cantor-like set (red)

EXAMPLE 3.4.1. Let $\mathbf{k}_\ell = \left(\frac{\ell+1}{4\ell+6}, \frac{2\ell+5}{8\ell+16}\right)$ for $\ell \geq 0$, and let F be the $\mathcal{F}$-limit set generated by the triple $(\mathcal{F}, \{\mathbf{k}_\ell\}_{\ell=0}^{\infty}, E_0)$. In Figure 3.1 we plot the usual Cantor set $\mathcal{C}$ (in blue) below the set F (in red) to illustrate the comparison. We can see that the set F has the same basic shape as the Cantor set $\mathcal{C}$, but is no longer strictly self-similar.

In order to compute the Hausdorff dimension of the new Cantor-like set F, we apply Corollary 3.10. Note that by equation (3.4.2),

$$\lim_{\ell\to\infty} ||\mathbf{L}_{\mathbf{k}_\ell}||_s = \lim_{\ell\to\infty} ||\mathbf{k}_\ell||_s = \frac{2^{\frac{1}{s}}}{4}.$$

So,

$$\underline{s_*} = \sup_s\{\liminf_{\ell\to\infty} ||\mathbf{L}_{\mathbf{k}_\ell}||_s > 1\} = \sup_s \left\{\frac{2^{\frac{1}{s}}}{4} > 1\right\} = \frac{1}{2}.$$

Similarly, we also have $\overline{s^*} = \frac{1}{2}$. By Corollary 3.10, $\dim_H(F) = \frac{1}{2}$. Here, F satisfies the uniform covering condition (3.1.4) since

$$\sup\left\{k_\ell^{(1)} + k_\ell^{(2)} : \ell = 0, 1, 2, \cdots\right\} = \frac{1}{2} < 1,$$

according to Proposition 3.16.

In the next example, we will construct a random Cantor-like set as follows.

Example 3.4.2. For each $\ell \geq 0$, we take $\mathbf{k}_\ell = \left(q_\ell, \frac{1}{2} - q_\ell\right)$ where q_ℓ is a random number between $\frac{1}{8}$ and $\frac{3}{8}$. Let F be the corresponding $\mathcal{F}$-limit set generated by the triple $(\mathcal{F}, \{\mathbf{k}_\ell\}_{\ell=0}^{\infty}, E_0)$. We plot the first few generations in Figure 3.2. In this example, the total length of the n^{th} generation $E^{(n)}$ is chosen to be $(\frac{1}{2})^n$, while the scaling factors of the left subintervals at each stage are randomly chosen.

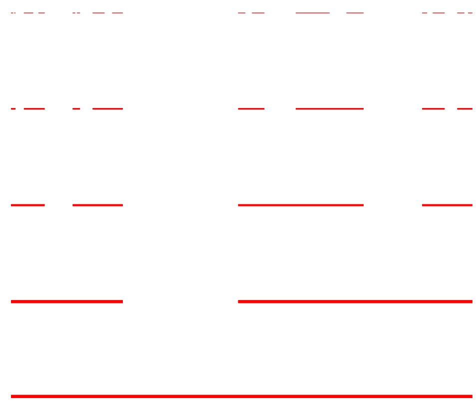

Figure 3.2. A randomly generated Cantor-like set

We now estimate the dimension of F. By (3.4.2),

$$\left(\frac{1}{8}, \frac{1}{8}\right) \leq \mathbf{L}_{\mathbf{k}_\ell} = \mathbf{k}_\ell = \mathbf{U}_{\mathbf{k}_\ell} \leq \left(\frac{3}{8}, \frac{3}{8}\right).$$

By Corollary 3.12,

$$\frac{\log(2)}{-\log(1/8)} \leq \dim_H(F) \leq \frac{\log(2)}{-\log(3/8)}.$$

That is,

$$\frac{1}{3} \leq \dim_H(F) \leq \frac{\log(2)}{\log(8/3)} \approx 0.7067.$$

Note that due to Proposition 3.16, F satisfies the uniform covering condition (3.1.4) since $q_\ell + \frac{1}{2} - q_\ell = \frac{1}{2} < 1$ for each $\ell \geq 0$.

Example 3.4.3. In this example, we create a sequence $\{\mathbf{k}_\ell\}_{\ell=0}^{\infty}$ that results in a limit set with a given measure, e.g. 1/3. Of course, the classic example of such a limiting set is the fat Cantor set. For a different approach, let $\sum_{n=0}^{\infty} a_n$ be any convergent series of positive terms with limit L. We consider a sequence $\{\mathbf{k}_\ell\}_{\ell=0}^{\infty}$ defined in the following way.

Let $n \geq 1$ be the generation of the construction and for each ℓ with $2^{n-1} - 1 \leq \ell \leq 2^n - 2$, define $\mathbf{k}_\ell = (b_n, b_n)$ where

$$b_1 := \frac{\frac{3}{2}L - a_0}{2\left(\frac{3}{2}L\right)} \qquad \text{and} \qquad b_n := \frac{\frac{3}{2}L - \sum_{i=0}^{n-1} a_i}{2\left(\frac{3}{2}L - \sum_{i=0}^{n-2} a_i\right)} \text{ for } n \geq 2.$$

With this sequence $\{\mathbf{k}_\ell\}_{\ell=0}^{\infty}$, one can find that the length of each interval in the n^{th} generation is

$$b_1 b_2 \cdots b_n = \frac{\frac{3}{2}L - \sum_{i=0}^{n-1} a_i}{2^n \cdot \frac{3}{2}L}.$$

Thus, the total length of the n^{th} generation is

$$\frac{\frac{3}{2}L - \sum_{i=0}^{n-1} a_i}{\frac{3}{2}L} = 1 - \frac{2}{3L}\sum_{i=0}^{n-1} a_i$$

which converges to $1/3$ as desired.

As an example, we take the convergent series $\displaystyle\sum_{n=0}^{\infty} \frac{1}{n!} = e$ and use it to create the $\mathcal{F}$-limit set F with measure $1/3$. The first few generations are shown in Figure 3.3.

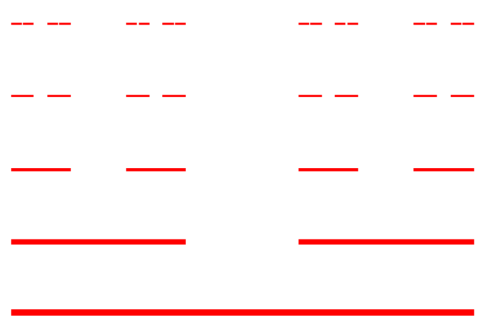

FIGURE 3.3. Fractal of measure $\frac{1}{3}$ created by using $\sum_{n=0}^{\infty} \frac{1}{n!} = e$

3.4.2. Sierpinski Triangle. The Sierpinski triangle is another well known fractal.

Following the general setup in Section 3.2, we take

$$\mathcal{X} = \{(A, B, C) \mid A, B, C \in \mathbb{R}^2\} \tag{3.4.3}$$

representing the collection of all triangles ΔABC in $\mathbb{R}^2$, $m = 3$, and $\mathcal{M} = [0,1]^6 \subseteq \mathbb{R}^6$. For each $\mathbf{k} = \left(k^{(1)}, k^{(2)}, k^{(3)}, k^{(4)}, k^{(5)}, k^{(6)}\right) \in \mathcal{M}$ and $i = 1,2,3$ we can define affine transformations $f_{\mathbf{k}}^{(i)} : \mathcal{X} \to \mathcal{X}$ as

$$\begin{aligned}
f_{\mathbf{k}}^{(1)}(A,B,C) &= (A, A + k^{(1)}(B-A), A + k^{(2)}(C-A)) \\
f_{\mathbf{k}}^{(2)}(A,B,C) &= (B + k^{(4)}(A-B), B, B + k^{(3)}(C-B)) \\
f_{\mathbf{k}}^{(3)}(A,B,C) &= (C + k^{(5)}(A-C), C + k^{(6)}(B-C), C)
\end{aligned}$$

for every $(A,B,C) \in \mathcal{X}$.

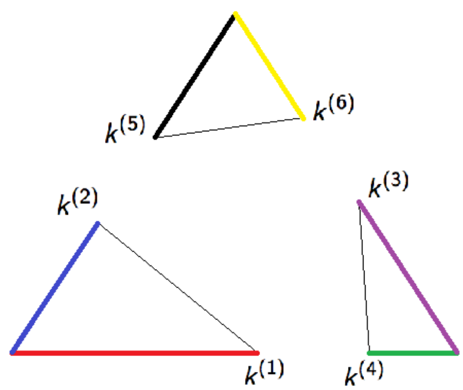

FIGURE 3.4. Geometric illustration of $\mathbf{k} \in \mathcal{M}$

Note that each $f_{\mathbf{k}}^{(i)}$ is a compression map for $i = 1,2,3$ and any $\mathbf{k} \in \mathcal{M}$. Thus, this defines a marking

$$\begin{aligned}
\mathcal{F}: \quad \mathcal{M} &\to \mathcal{C}_3(\mathcal{X}) \\
\mathbf{k} &\mapsto f_{\mathbf{k}} = (f_{\mathbf{k}}^{(1)}, f_{\mathbf{k}}^{(2)}, f_{\mathbf{k}}^{(3)}).
\end{aligned}$$

Of course, to prevent overlaps we can require that $k^{(1)} + k^{(4)} \leq 1, k^{(2)} + k^{(5)} \leq 1, k^{(3)} + k^{(6)} \leq 1$. When each of the inequalities are strict, the images of $f_{\mathbf{k}}^{(i)}$ are three disconnected triangles, as illustrated in Figure 3.5a. When all equalities hold, the images are connected, as illustrated in Figure 3.5b.

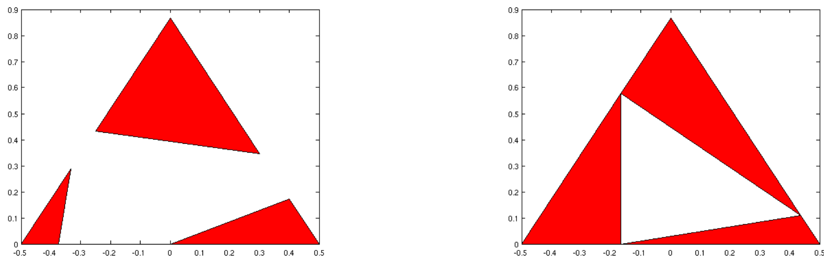

(A) (B)

FIGURE 3.5. First generation of disconnected and connected triangles

In the case of the connected sets, the values of $\mathbf{k} = \left(k^{(1)}, k^{(2)}, k^{(3)}, k^{(4)}, k^{(5)}, k^{(6)}\right)$ are determined by $k^{(1)}, k^{(2)}, k^{(3)}$ since $k^{(4)} = 1 - k^{(1)}$, $k^{(5)} = 1 - k^{(2)}$, $k^{(6)} = 1 - k^{(3)}$. In this case, we may also view $\mathbf{k} = \left(k^{(1)}, k^{(2)}, k^{(3)}\right)$ as a vector in $[0, 1]^3 \subseteq \mathbb{R}^3$.

To create the normal Sierpinski triangle, we choose

$$E_0 = \begin{bmatrix} -1/2 & 1/2 & 0 \\ 0 & 0 & \sqrt{3}/2 \end{bmatrix}, \tag{3.4.4}$$

the equilateral triangle of unit side length, and $\mathbf{k}_\ell \in \mathcal{M}$ to be the constant sequence $\mathbf{k}_\ell = \mathbf{k} = (1/2, 1/2, 1/2, 1/2, 1/2, 1/2)$ so that each iteration maps a triangle to three triangles of half the side length with the desired translation. In this case the $\mathcal{F}$-limit set generated by $(\mathcal{F}, \{\mathbf{k}_\ell\}_{\ell=0}^{\infty}, E_0)$ corresponds to the standard Sierpinski Triangle, as seen in Figure 1.7.

To generate Sierpinski-like fractals, we now adjust the values of the marking parameters $\{\mathbf{k}_\ell\}_{\ell=0}^{\infty}$. For each $\mathbf{k} = (k^{(1)}, k^{(2)}, \cdots, k^{(6)}) \in \mathcal{M}$ and $1 \leq i \leq 3$,

$$U\left(f_{\mathbf{k}}^{(i)}\right) = \sup_{(A,B,C)\in\mathcal{X}} \frac{diam\left(f_{\mathbf{k}}^{(i)}(A, B, C)\right)}{diam\left((A, B, C)\right)} = \max\left\{k^{(2i-1)}, k^{(2i)}\right\},$$

and

$$L\left(f_{\mathbf{k}}^{(i)}\right) = \inf_{(A,B,C)\in\mathcal{X}} \frac{diam\left(f_{\mathbf{k}}^{(i)}(A, B, C)\right)}{diam\left((A, B, C)\right)} = \min\left\{k^{(2i-1)}, k^{(2i)}\right\}.$$

When $\mathbf{k}$ is bounded, i.e. if $\lambda \leq k^{(j)} \leq \Lambda < 1$ for all $j = 1, \cdots, 6$, then

$$\mathbf{U}_{\mathbf{k}} \leq \mathbf{r} := (r, \cdots, r) \text{ and } \mathbf{L}_{\mathbf{k}} \geq \mathbf{s} := (s, \cdots, s),$$

where $r = \max\{1-\lambda, \Lambda\}$ and $s = \min\{1-\lambda, \Lambda\}$.

Following our general process, we construct some random Sierpinski-like sets by introducing randomness into the choice of the sequence $\{\mathbf{k}_\ell\}_{\ell=0}^{\infty}$.

Example 3.4.4. Let $\{\mathbf{k}_\ell\}_{\ell=0}^{\infty} = \left\{\left(k_\ell^{(1)}, k_\ell^{(2)}, k_\ell^{(3)}\right)\right\}_{\ell=0}^{\infty}$ be a sequence in $[0,1]^3$ with each $k_\ell^{(i)}$ a random number between given numbers λ and Λ for each $i = 1, 2, 3$. Let F be the $\mathcal{F}$-limit set generated by $(\mathcal{F}, \{\mathbf{k}_\ell\}_{\ell=0}^{\infty}, E_0)$. Then the 6^{th} generation of the construction results in images like Figure 3.6. Here, in Figure 3.6a, $\lambda = \frac{1}{4}$ and $\Lambda = \frac{3}{4}$; while in Figure 3.6b, $\lambda = 0.45$ and $\Lambda = 0.55$. Note that the sets are no longer self-similar.

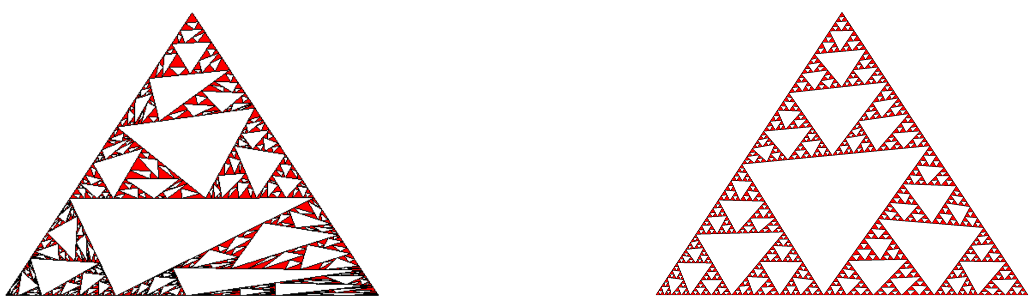

(a) Each $k_\ell^{(i)}$ is random in $[\frac{1}{4}, \frac{3}{4}]$.

(b) Each $k_\ell^{(i)}$ is random in $[0.45, 0.55]$.

Figure 3.6. Generation 6 of Random Sierpinski triangle

In Figure 3.6b, we pick $\lambda = 0.45$ and $\Lambda = 0.55$. By Corollary 3.12,

$$\frac{\log(m)}{-\log(s)} \le \dim_H(F) \le \frac{\log(m)}{-\log(r)},$$

where $m = 3$, $r = 0.55$ and $s = 0.45$. That is,

$$1.3758 \le \dim_H(F) \le 1.8377,$$

provided F satisfies the uniform covering condition (3.1.4).

Example 3.4.5. As in Example 3.4.4, but replacing E_0 with $\tilde{E_0} = \begin{bmatrix} 0 & 1 & 0 \\ 0 & 0 & 1 \end{bmatrix}$, the 7^{th} generation of the construction results in an image like Figure 3.7, when $\lambda = \frac{1}{4}$ and $\Lambda = \frac{3}{4}$.

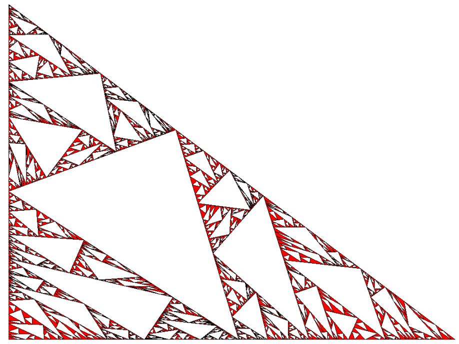

FIGURE 3.7. Generation 7 of a Random Sierpinski triangle

EXAMPLE 3.4.6. For each $\ell = 0, 1, \cdots$, let $\mathbf{k}_\ell = \left(k_\ell^{(1)}, k_\ell^{(2)}, \cdots, k_\ell^{(6)}\right)$ where

$$\begin{aligned}
k_\ell^{(1)} &= \frac{1}{2} + \frac{a_\ell}{\sqrt{\ell+1}}, \quad k_\ell^{(2)} = 1 - k_\ell^{(1)}, \\
k_\ell^{(3)} &= \frac{1}{2} + \frac{b_\ell}{\sqrt{\ell+1}}, \quad k_\ell^{(4)} = 1 - k_\ell^{(3)}, \\
k_\ell^{(5)} &= \frac{1}{2} + \frac{c_\ell}{\ell+1}, \quad k_\ell^{(6)} = 1 - k_\ell^{(5)}.
\end{aligned}$$

for random numbers $a_\ell, b_\ell, c_\ell \in [-\frac{1}{3}, \frac{1}{3}]$. Let F be the $\mathcal{F}$-limit set F generated by $(\mathcal{F}, \{\mathbf{k}_\ell\}_{\ell=0}^{\infty}, E_0)$. Then the seventh generation of the construction of F results in an image like Figure 3.8.

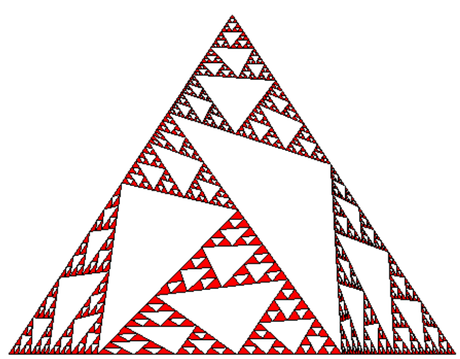

FIGURE 3.8. Generation 6 of a Sierpinski-type triangle with controlled dimension

In this case, we can calculate the exact value of the Hausdorff dimension of F. Indeed, by Corollary 3.10,

$$\lim_{\ell\to\infty}(||\mathbf{U}_{\mathbf{k}_\ell}||_s)^s = \frac{3}{2^s} = \lim_{\ell\to\infty}(||\mathbf{L}_{\mathbf{k}_\ell}||_s)^s.$$

Thus, $\dim_H(F) = \frac{\log(3)}{\log(2)}$, provided F satisfies the uniform covering condition (3.1.4).

3.4.3. Menger Sponge. Let

$$\mathcal{X} = \left\{(O, A, B, C) \mid O, A, B, C \in \mathbb{R}^3\right\} \tag{3.4.5}$$

representing the collection of all rectangular prisms $(OABC)$ in $\mathbb{R}^3$, $m = 20$, and

$$\mathcal{M} = \left\{\left(k^{(1)}, k^{(2)}, k^{(3)}, k^{(4)}, k^{(5)}, k^{(6)}\right) \in [0,1]^6 : k^{(1)} \le k^{(2)}, k^{(3)} \le k^{(4)}, k^{(5)} \le k^{(6)}\right\}. \tag{3.4.6}$$

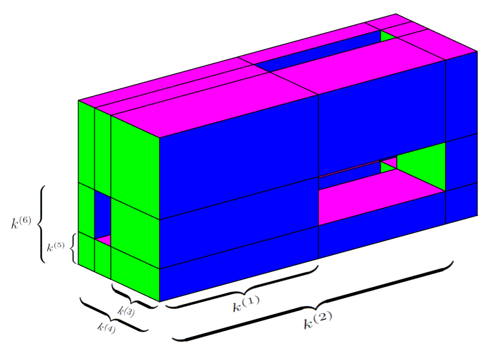

FIGURE 3.9. Geometric illustration of $\mathbf{k} \in \mathcal{M}$

For each $\mathbf{k} \in \mathcal{M}$ and $i = 1, 2, \ldots, 20$, we can define affine transformations $f_{\mathbf{k}}^{(i)} : \mathcal{X} \to \mathcal{X}$ as follows.

For any $\mathbf{k} = (k^{(1)}, k^{(2)}, k^{(3)}, k^{(4)}, k^{(5)}, k^{(6)}) \in \mathcal{M}$, define

$$T = \begin{bmatrix} 0 & k^{(1)} & k^{(2)} & 1 \end{bmatrix}, \quad R = \begin{bmatrix} 0 & k^{(3)} & k^{(4)} & 1 \end{bmatrix}, \quad S = \begin{bmatrix} 0 & k^{(5)} & k^{(6)} & 1 \end{bmatrix}.$$

Let

$$I \quad = \quad \{(a, b, c) \mid 1 \le a, b, c \le 3 \text{ with } a, b, c \in \mathbb{Z}, \text{and no two of } a, b, c \text{ equal to } 2\}.$$

For each $(a, b, c) \in I$ and $\mathbf{k} \in \mathcal{M}$, define

$$M_{\mathbf{k}}(a,b,c) = \begin{bmatrix} 1-(T(a)+R(b)+S(c)) & T(a) & R(b) & S(c) \\ 1-(T(a+1)+R(b)+S(c)) & T(a+1) & R(b) & S(c) \\ 1-(T(a)+R(b+1)+S(c)) & T(a) & R(b+1) & S(c) \\ 1-(T(a)+R(b)+S(c+1)) & T(a) & R(b) & S(c+1) \end{bmatrix}.$$

Note that the set I contains 20 elements, so we can express it as

$$I = \{(a_i, b_i, c_i) \mid 1 \le i \le 20\}.$$

For each $\mathbf{k} \in \mathcal{M}$ and $1 \le i \le 20$, we consider the affine transformation $f_{\mathbf{k}}^{(i)} : \mathcal{X} \to \mathcal{X}$ given by

$$f_{\mathbf{k}}^{(i)}(O,A,B,C) = M_{\mathbf{k}}(a_i,b_i,c_i) \begin{bmatrix} O \\ A \\ B \\ C \end{bmatrix} \tag{3.4.7}$$

for every $(O,A,B,C) \in \mathcal{X}$.

Note that for $i = 1,\ldots,20$ and $\mathbf{k} \in \mathcal{M}$, $f_{\mathbf{k}}^{(i)}$ is a compression. Thus, we can define a marking $\mathcal{F}$ by

$$\begin{aligned} \mathcal{F}: \quad \mathcal{M} &\to \mathcal{C}_{20}(\mathcal{X}) \\ \mathbf{k} &\mapsto f_{\mathbf{k}} = (f_{\mathbf{k}}^{(1)},\ldots,f_{\mathbf{k}}^{(20)}). \end{aligned}$$

Using this, for any starting rectangular prism $E_0 = (O,A,B,C) \in \mathcal{X}$, we can generate a sequence of sets that follows a similar construction to the Menger Sponge.

Example 3.4.7. Let

$$E_0 = \begin{bmatrix} 0 & 1 & 0 & 0 \\ 0 & 0 & 1 & 0 \\ 0 & 0 & 0 & 1 \end{bmatrix} \tag{3.4.8}$$

be the cube of unit side length and choose $\mathbf{k}_\ell \in \mathcal{M}$ to be the constant sequence $\mathbf{k}_\ell = \mathbf{k} = (1/3, 2/3, 1/3, 2/3, 1/3, 2/3)$. Then the $\mathcal{F}$-limit set F generated by the triple $(\mathcal{F}, \{\mathbf{k}_\ell\}_{\ell=0}^{\infty}, E_0)$ is the classical Menger sponge, as seen in Figure 1.8.

Now we consider variations of Menger Sponge. For each $\mathbf{k} = (k^{(1)}, k^{(2)}, \cdots, k^{(6)}) \in \mathcal{M}$ and $1 \leq i \leq 20$,

$$\begin{aligned} U\left(f_{\mathbf{k}}^{(i)}\right) &= \sup_{(O,A,B,C)\in\mathcal{X}} \frac{diam\left(f_{\mathbf{k}}^{(i)}(O,A,B,C)\right)}{diam\left((O,A,B,C)\right)} \\ &= \sup_{(O,A,B,C)\in\mathcal{X}} \frac{diam\left(M_{\mathbf{k}}(a_i,b_i,c_i)[O,A,B,C]'\right)}{diam\left((O,A,B,C)\right)} \\ &= \max\{T(a_{i+1})-T(a_i), R(b_{i+1})-R(b_i), S(c_{i+1})-S(c_i)\}. \end{aligned}$$

Similarly,

$$L\left(f_{\mathbf{k}}^{(i)}\right) = \min\{T(a_{i+1})-T(a_i), R(b_{i+1})-R(b_i), S(c_{i+1})-S(c_i)\}.$$

When $k^{(2j)} = 1 - k^{(2j-1)}$ for each $j = 1, 2, 3$, it is easy to check that

$$\begin{aligned} \sum_{i=1}^{20} U(f_{\mathbf{k}}^{(i)})^s &= \sum_{i=1}^{20} \max\{T(a_{i+1})-T(a_i), R(b_{i+1})-R(b_i), S(c_{i+1})-S(c_i)\}^s \\ &= 8\max\{k^{(1)}, k^{(3)}, k^{(5)}\}^s + 4\max\{1-2k^{(1)}, k^{(3)}, k^{(5)}\}^s \\ &\quad +4\max\{k^{(1)}, 1-2k^{(3)}, k^{(5)}\}^s + 4\max\{k^{(1)}, k^{(3)}, 1-2k^{(5)}\}^s. \end{aligned}$$

Example 3.4.8. Let

$$\tilde{E_0} = \begin{bmatrix} 0 & 3 & 0 & 0 \\ 0 & 0 & 1 & 0 \\ 0 & 0 & 0 & 2 \end{bmatrix}.$$

Let $\left(k^{(1)}, k^{(2)}, k^{(3)}, k^{(4)}, k^{(5)}, k^{(6)}\right) \in \mathcal{M}$ where each $k^{(i)}$ is a random number in $[0, 1]$, but still satisfying the condition $k^{(1)} \leq k^{(2)}, k^{(3)} \leq k^{(4)}, k^{(5)} \leq k^{(6)}$. Then the first generation $E^{(1)}$ of the construction results in a set like Figure 3.10.

Example 3.4.9. Let $\mathbf{k}_\ell = \left(k_\ell^{(1)}, k_\ell^{(2)}, k_\ell^{(3)}, k_\ell^{(4)}, k_\ell^{(5)}, k_\ell^{(6)}\right) \in \mathcal{M}$ with each $k_\ell^{(2j-1)}$ a random number between given parameters λ and Λ and $k_\ell^{(2j)} = 1 - k_\ell^{(2j-1)}$ for each $j = 1, 2, 3$. Let F be

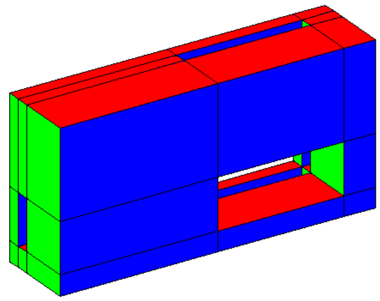

FIGURE 3.10. First generation of a randomly generated Menger sponge

the $\mathcal{F}$-limit set generated by $(\mathcal{F}, \{\mathbf{k}_\ell\}_{\ell=0}^{\infty}, E_0)$. Then the third iteration of the construction of F results in images like Figure 3.11. Here, in Figure 3.11a the parameters $\lambda = 0$ and $\Lambda = \frac{1}{2}$, while in Figure 3.11b the parameters $\lambda = 0.32$ and $\Lambda = 0.35$.

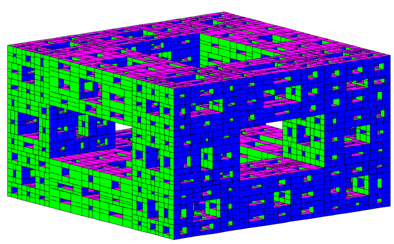

(A) $\lambda = 0, \quad \Lambda = \frac{1}{2}$

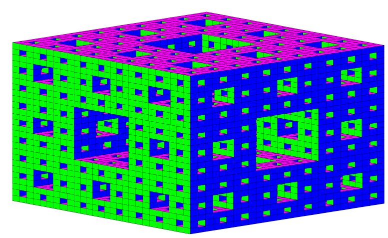

(B) $\lambda = 0.32, \Lambda = 0.35$

FIGURE 3.11. Generation 3 of random Menger sponge

We now calculate the dimension of the limit fractal F illustrated by Figure 3.11b in Example 3.4.9. Note that in general, when $\lambda \leq k^{(2j-1)} \leq \Lambda$ for each $j = 1, 2, 3$, it follows that

$$(||\mathbf{U}_\mathbf{k}||_s)^s = \sum_{i=1}^{20} U\left(f_\mathbf{k}^{(i)}\right)^s \leq 8\Lambda^s + 12\max\{1 - 2\lambda, \Lambda\}^s.$$

Similarly,

$$(||\mathbf{L}_\mathbf{k}||_s)^s \geq 8\lambda^s + 12\min\{1 - 2\Lambda, \lambda\}^s.$$

In particular, when $\lambda = 0.32$ and $\Lambda = 0.35$, for any $s > 2.901$,

$$\begin{aligned}(||\mathbf{U}_{\mathbf{k}}||_s)^s &\leq 8\Lambda^s + 12\max\{1-2\lambda, \Lambda\}^s \leq 8 * 0.35^s + 12 * 0.36^s \\ &< 8 * 0.35^{2.901} + 12 * 0.36^{2.901} \approx 1.000.\end{aligned}$$

By Theorem 3.8, $\dim_H(F) \leq 2.901$. Similarly, for any $s \leq 2.546$,

$$\begin{aligned}(||\mathbf{L}_{\mathbf{k}}||_s)^s &\geq 8\lambda^s + 12\min\{1-2\Lambda, \lambda\}^s \\ &\geq 8 * 0.32^s + 12 * 0.3^s \geq 8 * 0.32^{2.546} + 12 * 0.3^{2.546} \approx 1.000.\end{aligned}$$

By Theorem 3.8 again, $\dim_H(F) \geq 2.546$, provided F satisfies the uniform covering condition (3.1.4). As a result,

$$2.546 \leq \dim_H(F) \leq 2.901.$$

EXAMPLE 3.4.10. For each $\ell \geq 0$, let $\mathbf{k}_\ell = \left(k_\ell^{(1)}, k_\ell^{(2)}, \cdots, k_\ell^{(6)}\right)$ where

$$\begin{aligned}k_\ell^{(1)} &= \frac{1}{3} + \frac{(-1)^\ell}{12(\ell+1)^2}, \quad k_\ell^{(2)} = 1 - k_\ell^{(1)}, \\ k_\ell^{(3)} &= \frac{1}{3} - \frac{(-1)^\ell}{6(\ell+1)^2}, \quad k_\ell^{(4)} = 1 - k_\ell^{(3)}, \\ k_\ell^{(5)} &= \frac{1}{3} + \frac{(-1)^\ell}{18(\ell+1)^2}, \quad k_\ell^{(6)} = 1 - k_\ell^{(5)}.\end{aligned}$$

Let F be the $\mathcal{F}$-limit set generated by $(\mathcal{F}, \{\mathbf{k}_\ell\}_{\ell=0}^\infty, E_0)$. Then the third generation of the construction of F leads to an image like Figure 3.12.

In this case, we can still calculate the exact Hasudorff dimension of F. By direct computation,

$$\lim_{\ell\to\infty}(||\mathbf{U}_{\mathbf{k}_\ell}||_s)^s = \frac{20}{3^s} = \lim_{\ell\to\infty}(||\mathbf{L}_{\mathbf{k}_\ell}||_s)^s.$$

Thus, by Corollary 3.10, $\dim_H(F) = \frac{\log(20)}{\log(3)} \approx 2.7268$, since F satisfies the uniform covering condition according to Example 3.5.3.

REMARK 3.14. We discuss similarities and differences of this construction with $V-$variable fractals created by Barnsley et al. in [**4**], [**5**].

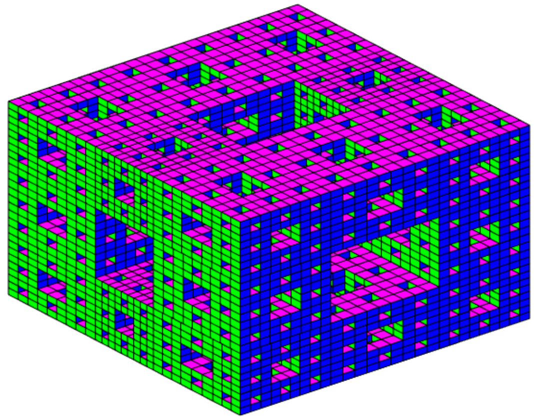

FIGURE 3.12. Generation 3 of random Menger sponge with controlled dimension

Barnsley, Hutchinson, and Stenflo have described a similar approach to creating more generalized fractals that can take on a prescribed amount of randomness. In [**4**] and [**5**], they describe a generating process for some fractals along with calculations of their dimensions. In essence, a V-variable fractal set has at most $V \in \mathbb{N}$ number of distinct patterns in each generation of the construction. This is done through the following process.

Let (X, d) be a metric space, Λ an index set, $F^\lambda = \{f_1^\lambda, f_2^\lambda, \ldots, f_m^\lambda\}$ an IFS for each $\lambda \in \Lambda$, and P a probability distribution on some σ-algebra of subsets of Λ. Then denote $\mathbf{F} = \{(X, d), F^\lambda, \lambda \in \Lambda, P\}$ to be a family of IFSs (with at least two functions in each IFS) defined on (X, d). Assume that the IFSs F^λ are *uniformly contractive* and *uniformly bounded*, that is, for some $0 < r < 1$,

$$\sup_\lambda \max_m d\left(f_m^\lambda(x), f_m^\lambda(y)\right) \leq r d(x, y), \tag{3.4.9}$$

$$\sup_\lambda \max_m d\left(f_m^\lambda(a), a\right) < \infty \tag{3.4.10}$$

for all $x, y \in X$ and some $a \in X$.

A *tree code* is a map ω from the set of all finite sequences $\{1, \ldots, m\}$ to Λ. A tree code is V-*variable* if for each positive integer k, there are at most V distinct tree codes in the tree truncated at the k^{th} generation. For example, consider the Sierpinski triangle. We let F be the IFS that maps the triangle to three copies of $1/2$ the size, as usual. Let G be the IFS that maps the initial triangle to three triangles that are $1/3$ the size, with the vertices shared with the initial set being the fixed points of the maps. See Figure 3.13 for the image of the initial step of each. Thus, $\mathbf{F} = \{(\mathbb{R}^2, d), \{F, G\}, P = (1/2, 1/2)\}$ is the family $\{F, G\}$ with probability function uniformly choosing 1/2 for each IFS. Using these IFSs, three V-variable pre-fractals are given in Figure 3.14, being 1-variable, 2-variable, and 3-variable respectively.

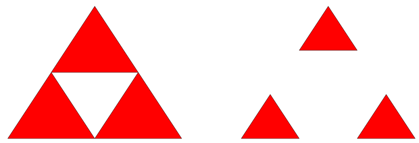

FIGURE 3.13. Initial steps of IFSs F and G respectively

Now, we express V-variable fractals in terms of $\mathcal{F}$-limit sets. Let $\mathcal{X}, \mathcal{M}, \mathcal{F}$ and E_0 be as in Section 3.4.2. Let $F = \left(\frac{1}{2}, \frac{1}{2}, \frac{1}{2}, \frac{1}{2}, \frac{1}{2}, \frac{1}{2}\right) \in \mathcal{M}$ and $G = \left(\frac{1}{3}, \frac{1}{3}, \frac{1}{3}, \frac{1}{3}, \frac{1}{3}, \frac{1}{3}\right) \in \mathcal{M}$. We will use F and G to denote terms in the sequence $\{k_\ell\}_{\ell=1}^{\infty}$. Consider the third generation examples in Figure 3.14.

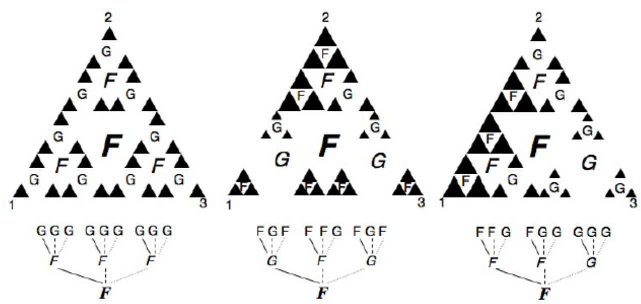

FIGURE 3.14. $n = 3$ generation prefractals that are 1, 2 and 3-variable respectively. Images from [**5**].

Then from left to right we have the following:

$$
\begin{aligned}
V = 1 \qquad \{k_\ell\}_{\ell=1}^{13} &= \{F, F, F, F, G, G, G, G, G, G, G, G, G\} \\
V = 2 \qquad \{k_\ell\}_{\ell=1}^{13} &= \{F, G, F, G, F, G, F, F, F, G, F, G, F\} \\
V = 3 \qquad \{k_\ell\}_{\ell=1}^{13} &= \{F, F, F, G, F, F, G, F, G, G, G, G, G\}.
\end{aligned}
$$

From these examples, we can see that if we want to create a V-variable fractal, for each generation we should choose at most V distinct triples from the set $\{(A, B, C) | A, B, C \in \{F, G\}\}$ and repeat those triples in any order.

When $V < \infty$, there are at most V distinct tree codes in the address of point in the set. We can create such a situation from our construction described earlier in Chapter 3 by choosing blocks of $\{k_\ell\}$ that repeat across generations. In the case that $V = \infty$, the fractal is based off of a probability distribution for applying specific IFSs. In our construction we also can use a probability distribution to determine the contraction ratios within a generation (as in Examples 3.4.2, 3.4.4 and 3.4.8), but we do not require such a choice. We allow for deterministic sequences that also do not repeat any blocks, thus not falling into the category of V-variable.

3.5. Uniform Covering Condition

In previous sections, we have seen that the uniform covering condition (3.1.4) plays a vital role in computing a lower estimate for the Hausdorff dimension of a fractal. In this section we explore the sufficient conditions needed for a fractal to satisfy the uniform covering condition.

PROPOSITION 3.15. *Let (X, d) be a metric space with the following property: For any $\epsilon > 0$, there exists a natural number N_ϵ such that for any $\rho > 0$, any closed ball in X of diameter ρ contains at most N_ϵ many disjoint balls of diameter $\epsilon\rho$. Clearly, any Euclidean space satisfies this property.*

Let $\mathcal{J} := \{J_\sigma : \sigma \in D\}$ be a collection of compact subsets of (X, d), and F be the limit set of $\mathcal{J}$ as given in (2.1.4). Suppose that $\mathcal{J}$ satisfies the following conditions:

(1) *there exists a number $r \in (0, 1]$ such that for any $k \in \mathbb{N}$ and for each $\sigma \in D_k$,*

$$rc_k \leq diam(J_\sigma) \leq \frac{c_k}{r}$$

where $c_k := \min\{diam(J_{\bar{\sigma}}) : \bar{\sigma} \in D_{k-1}\}$.

(2) *there exists a number $\tau \in (0, 1]$ such that for each $\sigma \in D$, the convex hull of J_σ contains a closed ball W_σ such that*

$$diam(W_\sigma) \geq \tau \cdot diam(J_\sigma)$$

and for each $k \in \mathbb{N}$, the collection $\{W_\sigma : \sigma \in D_k\}$ are pairwise disjoint.

Then F satisfies the uniform covering condition (3.1.4).

Proof. For any closed ball B in X, let k be the number such that

$$c_{k+1} \leq diam(B) < c_k$$

where by convention, we set $c_0 = \infty$. Let

$$D_B := \{\sigma \in D_k : B \cap F \cap J_\sigma \neq \emptyset\}.$$

Note that

$$B \cap F = B \cap F \cap \bigcup_{\sigma \in D_k} J_\sigma \subseteq \bigcup_{\sigma \in D_B} J_\sigma.$$

Also for any $\sigma \in D_B$, since $diam(J_\sigma) \leq \frac{c_k}{r}$ and $B \cap J_\sigma \neq \emptyset$, it follows that $J_\sigma \subseteq \bar{B}(x_0, \frac{r+2}{2r}c_k)$, where $x_0 \in X$ is the center of the ball B. Thus, $W_\sigma \subseteq \bar{B}(x_0, \frac{r+2}{2r}c_k)$. Let $\rho = \frac{r+2}{r}c_k$ and $\epsilon = \frac{r^2}{r+2}\tau$, then

$$diam(W_\sigma) \geq \tau \cdot diam(J_\sigma) \geq \tau r c_k = \epsilon\rho.$$

Since $\{W_\sigma : \sigma \in D_B\}$ are pairwise disjoint, the cardinality of D_B is at most $N := N_\epsilon$.

On the other hand, for $\gamma = \frac{r^2}{N}$, it holds that

$$diam(B) \geq c_{k+1} \geq rc_k = \gamma N \frac{c_k}{r} \geq \gamma \sum_{\sigma \in D_B} \frac{c_k}{r} \geq \gamma \sum_{\sigma \in D_B} diam(J_\sigma). \tag{3.5.1}$$

As a result, $\mathcal{J}$ satisfies the condition (3.1.4) as desired. □

We now discuss some specific sufficient conditions concerning the types of examples provided in section 3.4. To start, let's first consider Cantor-like constructions. Let X be the family of closed intervals described in (3.4.1), $m = 2$, and $\mathcal{M} = [0, 1]^2 \subseteq \mathbb{R}$.

Proposition 3.16. *Let $\{\mathbf{k}_\ell\}_{\ell=0}^\infty$ be a sequence in $\mathcal{M}$ with*

$$\sup\left\{k_\ell^{(1)} + k_\ell^{(2)} : \ell = 0, 1, 2, \cdots\right\} < 1,$$

and F be the $\mathcal{F}$-limit set generated by the triple $(\mathcal{F}, \{\mathbf{k}_\ell\}_{\ell=0}^\infty, E_0)$. Then F satisfies the uniform covering condition (3.1.4).

Proof. Let $N = 1$ and

$$\gamma = \inf_{\ell} \left\{ 1 - k_\ell^{(1)} - k_\ell^{(2)} \right\} \in (0, 1]. \tag{3.5.2}$$

For any closed interval B in $\mathbb{R}$ with $B \cap F \neq \emptyset$, consider the set

$$\mathcal{L} := \{\ell(\sigma) : B \cap F \subseteq J_\sigma, \sigma \in D\},$$

where $\ell(\sigma)$ is given in (3.3.3). Note that $\mathcal{L}$ is nonempty because $B \cap F \subseteq J_0$ implies that $\ell(0) \in \mathcal{L}$.

If $\mathcal{L}$ is an infinite set, then since $diam(J_\sigma) \to 0$ as $\ell(\sigma) \to \infty$, there exists $\sigma^* \in D$ such that $\ell(\sigma^*) \in \mathcal{L}$ and $diam(B) \geq diam(J_{\sigma^*}) \geq \gamma \cdot diam(J_{\sigma^*})$.

If $\mathcal{L}$ is finite, let $\ell(\sigma^*)$ be the maximum number in $\mathcal{L}$ for some $\sigma^* \in D$. Then, $\ell(\sigma^*) \in \mathcal{L}$ but $\ell(\sigma^* * j) \notin \mathcal{L}$ for each $j = 1, 2$. This implies that $B \cap J_{\sigma^* * j} \neq \emptyset$ for both $j = 1, 2$ because $J_{\sigma^*} = J_{\sigma^* * 1} \cup J_{\sigma^* * 2}$. Since B is an interval, the gap $J \setminus (J_{\sigma^* * 1} \cup J_{\sigma^* * 2})$ between $J_{\sigma^* * 1}$ and $J_{\sigma^* * 2}$ is contained in B, which yields that

$$\begin{aligned} diam(B) &\geq diam\left(J \setminus (J_{\sigma^* * 1} \cup J_{\sigma^* * 2})\right) \\ &= diam(J) - diam(J_{\sigma^* * 1}) - diam(J_{\sigma^* * 2}) \\ &\geq diam(J_{\sigma^*}) \left(1 - k_{\ell(\sigma^*)}^{(1)} - k_{\ell(\sigma^*)}^{(2)}\right) \geq \gamma \cdot diam(J_{\sigma^*}). \end{aligned}$$

As a result, in both cases, the uniform covering condition (3.1.4) holds. □

Motivated by Proposition 3.16, we now consider a generalization of the above result.

Definition 3.17. Let $n \geq 1$ and $\mathcal{H}$ be a collection of subsets of a metric space (X, d). Define

$$\rho_n(\mathcal{H}) = \inf\{r : \text{There exists a ball } B \text{ in } X \text{ of radius } r \text{ that intersects at least } n+1 \text{ elements in } \mathcal{H}\}. \tag{3.5.3}$$

Here $\rho_n(\mathcal{H})$ is a quantity describing the "gap" between $n + 1$ elements of $\mathcal{H}$.

Definition 3.18. Let $\mathcal{J} = \{J_\sigma : \sigma \in D\}$ be a collection of compact subsets of a metric space (X, d), and $n \geq 1$. Define

$$\gamma_n(\mathcal{J}) := \inf \left\{ \frac{\rho_n(\{J_{\sigma*i} : \sigma \in R_k, i = 1, 2, \cdots, m\})}{\sum_{\sigma \in R_k} diam(J_\sigma)} : \text{ for some } k \right. \\ \left. \text{and } R_k \subseteq D_k \text{ with } 1 \leq |R_k| \leq n \right\}, \tag{3.5.4}$$

where $|R_k|$ denotes the cardinality of the set R_k. Here $\gamma_n(\mathcal{J})$ is a quantity describing the relative size of the "gap" between $n+1$ children of a generation and the size of the parent sets.

Now we give some examples of calculations of these two quantities.

Example 3.5.1. Let $\mathcal{J}$ be the collection of closed intervals used in the construction of a Cantor-like set given in (3.4.1). Then

$$\begin{aligned} \gamma_1(\mathcal{J}) &= \inf \left\{ \frac{\rho_1(\{J_{\sigma*i} : \sigma \in R_k, i = 1, 2\})}{diam(J_\sigma)} : \text{ for some } k \text{ and } R_k \subseteq D_k \text{ with } |R_k| = 1 \right\} \\ &= \inf \left\{ \frac{\rho_1(\{J_{\sigma*1}, J_{\sigma*2}\})}{diam(J_\sigma)} : \text{ for } \sigma \in D \right\} \\ &= \inf \left\{ \frac{diam(J_\sigma) - diam(J_{\sigma*1}) - diam(J_{\sigma*2})}{diam(J_\sigma)} : \sigma \in D \right\} \\ &= \inf \left\{ 1 - \frac{diam(J_{\sigma*1})}{diam(J_\sigma)} - \frac{diam(J_{\sigma*2})}{diam(J_\sigma)} : \sigma \in D \right\}, \end{aligned}$$

which agrees with the γ in (3.5.2), see Figure 3.15.

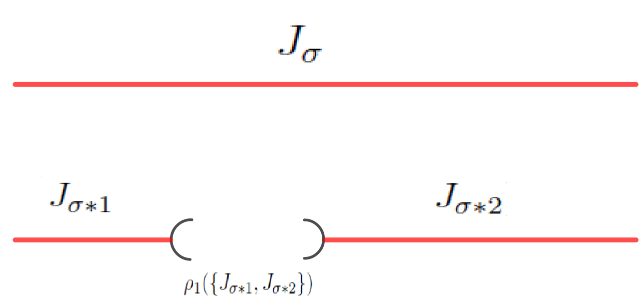

Figure 3.15. Illustration of $\rho_1(\{J_{\sigma*1}, J_{\sigma*2}\})$

Example 3.5.2. Let $\mathcal{J}$ be the collection of triangles used in (3.4.3). In the following figures, we plot the smallest ball that intersects a certain number of children. The children that have non-empty intersection with the ball are colored red, while those that have empty intersection are light blue.

First note that for any $\sigma \in D$, $\rho_1(\{J_{\sigma*1}, J_{\sigma*2}, J_{\sigma*3}\}) = 0$ since any pair of children share a vertex. At the intersection of the two children of J_σ one can construct a ball of arbitrarily small radius. See Figure 3.16.

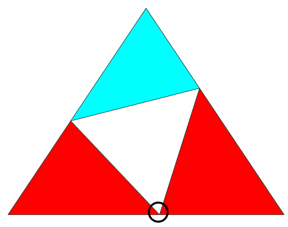

Figure 3.16. Illustration of $\rho_1(\{J_{\sigma*1}, J_{\sigma*2}, J_{\sigma*3}\}) = 0$

Moreover, $\rho_2(\{J_{\sigma*1}, J_{\sigma*2}, J_{\sigma*3}\}) > 0$ because the radius of any ball that intersects all three children of J_σ is bounded below by the radius of the inscribed circle of the removed center triangle. In other words, $\rho_2(\{J_{\sigma*1}, J_{\sigma*2}, J_{\sigma*3}\})$ is equal to the radius of the inscribed circle. See Figure 3.17 for illustration.

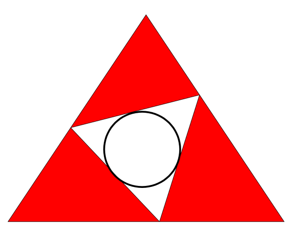

Figure 3.17. $\rho_2(\{J_{\sigma*1}, J_{\sigma*2}, J_{\sigma*3}\})$ = radius of inscribed circle

Now we may compute $\gamma_n(\mathcal{J})$ as follows.

Note that for $n = 1$,

$$\begin{aligned}\gamma_1(\mathcal{J}) &= \inf\left\{\frac{\rho_1(\{J_{\sigma*i} : \sigma \in R_k, i = 1,2,3\})}{diam(J_\sigma)} : \text{ for some } k \text{ and } R_k \subseteq D_k \text{ with } |R_k| = 1\right\}\\ &= \inf\left\{\frac{\rho_1(\{J_{\sigma*1}, J_{\sigma*2}, J_{\sigma*3}\})}{diam(J_\sigma)} : \text{ for } \sigma \in D\right\} = 0.\end{aligned}$$

On the other hand, when $n = 2$, we have

$$\gamma_2(\mathcal{J}) = \inf\left\{\frac{\rho_2(\{J_{\sigma*i} : \sigma \in R_k, i = 1,2,3\})}{diam(J_\sigma)} : \text{ for some } k \text{ and } R_k \subseteq D_k \text{ with } |R_k| \leq 2\right\}.$$

When $|R_k| = 1$, this is reduced to the same case as Figure 3.17.

When $|R_k| = 2$, we use two parent triangles, and must find the ball with smallest radius that intersects three or more children. See Figure 3.18 for a few candidates for the ball with smallest radius.

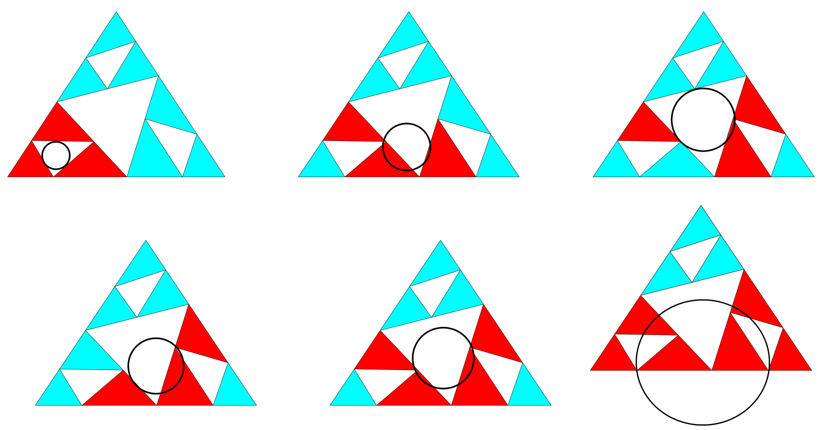

FIGURE 3.18. Various options for smallest radius ball

For each $R_k \subseteq D_k$ with $|R_k| \leq 2$, $\rho_2(\{J_{\sigma*i} : \sigma \in R_k, i = 1,2,3\}) > 0$. For some nice $\mathcal{J}$, one may expect $\gamma_2(\mathcal{J})$ to also be positive.

THEOREM 3.19. *Let $\mathcal{J} := \{J_\sigma : \sigma \in D\}$ be a collection of compact subsets of (X, d) satisfying MSC(3) and*

$$\lim_{k\to\infty} \max\{diam(J_\sigma) : \sigma \in D_k\} = 0,$$

and let F be the limit set of $\mathcal{J}$ as given in (2.1.4). If there exists an N such that $\gamma_N(\mathcal{J}) > 0$, then F satisfies the uniform covering condition (3.1.4).

Proof. Let $\gamma = \gamma_N(\mathcal{J}) > 0$. For any closed ball B in X with $B \cap F \neq \emptyset$, let $g(k)$ be the number of elements σ in D_k such that $B \cap F \cap J_\sigma \neq \emptyset$. Then $g : \mathbb{N} \cup \{0\} \to \mathbb{N}$ is monotone increasing with $g(0) = 1$.

Case 1: If $g(k) \leq N$ for all $k = 0, 1, 2, \cdots$, that is, for each k, there exists an index set I_k with $|I_k| \leq N$ such that $B \cap F \subseteq \bigcup_{i \in I_k} J_{\sigma_i^{(k)}}$ for some $\sigma_i^{(k)} \in D_k$. Thus when k is large enough,

$$diam(B) > \gamma \cdot \sum_{i \in I_k} diam(J_{\sigma_i^{(k)}})$$

due to the fact that

$$0 \leq \lim_{k \to \infty} \sum_{i \in I_k} diam(J_{\sigma_i^{(k)}}) \leq N \cdot \lim_{k \to \infty} \max\{diam(J_\sigma) : \sigma \in D_k\} = 0.$$

Hence, equation (3.1.4) holds for B.

Case 2: There exists $k^* \geq 0$ such that $g(k^*) \leq N$ but $g(k^* + 1) > N$.

Since $g(k^*) \leq N$, there are $g(k^*)$ many elements $\sigma \in D_{k^*}$ such that $B \cap F \cap J_\sigma \neq \emptyset$. That is, there exists $R_{k^*} \subseteq D_{k^*}$ with $|R_{k^*}| \leq N$ such that $B \cap F \subseteq \bigcup_{\sigma \in R_{k^*}} J_\sigma$. On the other hand, since $g(k^* + 1) > N$, $B \cap F$ intersects at least $N + 1$ elements of D_{k^*+1}. Since $B \cap F \subseteq \bigcup_{\sigma \in R_{k^*}} J_\sigma$, all of these $N + 1$ elements must be children of $\{J_\sigma : \sigma \in R_{k^*}\}$. Then, by the definition of ρ_N in (3.5.3),

$$diam(B) \geq \rho_N(\{J_{\sigma * i} : \sigma \in R_{k^*}, i = 1, 2, \ldots m\}) \geq \gamma \cdot \sum_{\sigma \in R_{k^*}} diam(J_\sigma). \tag{3.5.5}$$

As a result, F satisfies the uniform covering condition (3.1.4). $\square$

To show an application of Theorem 3.19, we now consider some examples provided in section 3.4.3.

Let $\{\mathbf{k}_\ell\}_{\ell=0}^\infty$ be a sequence in $\mathcal{M}$ as defined in (3.4.6) and F be the $\mathcal{F}-$limit set generated by $(\mathcal{F}, \{\mathbf{k}_\ell\}_{\ell=0}^\infty, E_0)$ associated with $\mathcal{J}(\vec{k}) = \{J_\sigma : \sigma \in D\}$ as defined in Definition 3.6. Let $\mathcal{H} \subseteq \mathcal{J}_k := \{J_\sigma : \sigma \in D_k\}$ for some $k \geq 0$, and consider $\rho_8(\mathcal{H})$.

We now make the following observation: *Suppose there exists a ball B that intersects at least 9 elements of $\mathcal{H}$. Then $diam(B)$ is greater than or equal to the smallest edge length of the elements* *in* $\mathcal{H}$*.* Indeed, by considering the projections to the three coordinate axes, one can see that at least one coordinate contains three non-identical projected images of these 9 elements. As a result the ball B intersected with these 9 elements will have a diameter at least the length of the smallest side of the three projected images. This proves our observation.

Let

$$m_\ell = \min\{k_\ell^{(1)}, k_\ell^{(2)} - k_\ell^{(1)}, 1 - k_\ell^{(2)}, k_\ell^{(3)}, k_\ell^{(4)} - k_\ell^{(3)}, 1 - k_\ell^{(4)}, k_\ell^{(5)}, k_\ell^{(6)} - k_\ell^{(5)}, 1 - k_\ell^{(6)}\} \tag{3.5.6}$$

and

$$M_\ell = \max\{k_\ell^{(1)}, k_\ell^{(2)} - k_\ell^{(1)}, 1 - k_\ell^{(2)}, k_\ell^{(3)}, k_\ell^{(4)} - k_\ell^{(3)}, 1 - k_\ell^{(4)}, k_\ell^{(5)}, k_\ell^{(6)} - k_\ell^{(5)}, 1 - k_\ell^{(6)}\}. \tag{3.5.7}$$

For any $\sigma \in D$, direct calculation shows that

$$m_{\ell(\sigma)} \leq \frac{diam(J_{\sigma * i})}{diam(J_\sigma)} \leq M_{\ell(\sigma)} \tag{3.5.8}$$

where $\ell(\sigma)$ is given in (3.3.3).

Thus, for any $\sigma = (i_1, i_2, \ldots, i_k) \in D_k$, we have

$$m_{\ell((i_1))} m_{\ell((i_1,i_2))} \cdots m_{\ell((i_1,\ldots,i_k))} \leq \frac{diam(J_\sigma)}{diam(J_\emptyset)} \leq M_{\ell((i_1))} M_{\ell((i_1,i_2))} \cdots M_{\ell((i_1,\ldots,i_k))}. \tag{3.5.9}$$

Let $R_k \subseteq D_k$ for some k. Suppose $|R_k| \leq 8$. Then for any $\sigma \in R_k$, by the observation

$$\begin{aligned}
& \frac{\rho_8(\{J_{\sigma * i} : \sigma \in R_k, i = 1, 2, \ldots 20\})}{\sum_{\sigma \in R_k} diam(J_\sigma)} \\
\geq\ & \frac{\text{smallest diameter of } J_{\sigma * i}}{8 \cdot \max\{diam(J_\sigma) : \sigma \in R_k\}} \\
\geq\ & \min\left\{ \frac{m_{\ell((i_1))} m_{\ell((i_1,i_2))} \cdots m_{\ell((i_1,\ldots,i_{k+1}))} diam(J_\emptyset)}{M_{\ell((i_1))} M_{\ell((i_1,i_2))} \cdots M_{\ell((i_1,\ldots,i_k))} diam(J_\emptyset)} : \sigma = (i_1, i_2, \ldots, i_k) \in R_k, i_{k+1} = 1, \ldots, 20 \right\} \\
\geq\ & \frac{1}{8} \left(\prod_{i=1}^{\infty} \frac{m_i}{M_i} \right) \liminf_{i \to \infty} m_i,
\end{aligned}$$

where the last inequality follows from $0 \leq m_i \leq M_i$ for each i.

EXAMPLE 3.5.3. Using this observation, we show that the $\mathcal{F}-$limit set in Example 3.4.10 satisfies the uniform covering condition. In this example,

$$m_\ell = \begin{cases} a_\ell & \ell \text{ even} \\ b_\ell & \ell \text{ odd} \end{cases} \text{ and } M_\ell = \begin{cases} b_\ell & \ell \text{ even} \\ a_\ell & \ell \text{ odd} \end{cases} \tag{3.5.10}$$

where

$$a_\ell = k_\ell^{(3)} = \frac{1}{3} - \frac{(-1)^\ell}{6(\ell+1)^2} \text{ and } b_\ell = 1 - 2k_\ell^{(3)} = \frac{1}{3} + \frac{(-1)^\ell}{3(\ell+1)^2}. \tag{3.5.11}$$

One may show that the product $\displaystyle\prod_{i=1}^{\infty} \frac{m_i}{M_i}$ is convergent, whose numerical value is 0.369761... and $\liminf_{i\to\infty} m_i = 1/3$. Thus $\gamma_8(\mathcal{J}) > 0$. Therefore, by Theorem 3.19, F satisfies the uniform covering condition.

APPENDIX A

Matlab Code for Figures

This appendix contains all the relevant Matlab code for generating the images of the modified (and original) Cantor, Sierpinski, and Menger fractals.

A.1. Cantor Set functions

```
function [A] = modcantor(N,P)
%P is the sequence of {k} coefficients
%draws the modified cantor set with given coefficients
if isempty(P)
P=ones(1,2^(N+1)-1)./3;
end
B=[0;1;0];
A=B;
k=0;


while k< N
newB=[];
for i=1:length(B(1,:))
j=length(A(1,:))+2*i-1;
C=[B(1,i) P(j)*(B(1,i)-B(2,i))+B(2,i);
P(j-1)*(B(2,i)-B(1,i))+B(1,i) B(2,i); k+1 k+1];
newB=[newB C];
end
```

```
B=newB;
A=[A B];
k=k+1;
end

figure
for i=1:length(A(1,:))
plot([A(1,i);A(2,i)],[A(3,i);A(3,i)],'r-',
'LineWidth',max(8/(A(3,i)+1),2))
axis off
hold on
end
end
```

```
for l=0:128
P(2*l+1)=(l+1)/(4*l+6);
P(2*l+2)=(2*l+5)/(8*l+16);
end


A=modcantor(6,P);
figure
for i=1:length(A(1,:))
plot([A(1,i);A(2,i)],[A(3,i);A(3,i)],'r-',
'LineWidth',max(8/(A(3,i)+1),2))
hold on
end
```

```
hold on
B=modcantor(6,ones(1,256)/3);
for i=1:length(B(1,:))
plot([B(1,i);B(2,i)],[B(3,i)-0.1;B(3,i)-0.1],'b-',
'LineWidth',max(8/(B(3,i)+1),2));
hold on
end
```

A.2. Sierpinski Triangle functions

```
function L = modsierpinski(X,N,ind)
%X is initial triangle vertices in 2x3 matrix
%N is number of generations wanted
%ind=index of type of fractal wanted:

%if index==0, creates usual sieprinski sequence
%if index==1, creates sierpinski dust type sequence
%if index==2, creates random, endpoint-connected sequence
%if index==3, creates random dust type sequence
%if index==4, creates convergent sequence to 1/2 scaling
%if index==5, creates convergent random sequence to 1/2 scaling

if isempty(X)
X=[-1/2 1/2 0; 0 0 sqrt(3)/2];
end

P=genP(N,ind);
%P=onevariable(N,ind);
L=X;
```

```
M=X;
for k=1:N
M=nextgen(L,k-1,P(3^k-2:3^(k+1)-3));
L=M;
end

figure
for j=1:length(M(:,1))/2
fill(M(2*j-1,:),M(2*j,:),'r');
hold on

end
end
```

```
function [P] = genP(N,ind)
%generates the sequence P of scaling ratios for all N generations
%if index==0, creates usual sieprinski sequence
%if index==1, creates sierpinski dust type sequence
%if index==2, creates random, endpoint-connected sequence
%if index==3, creates random dust type sequence
%if index==4, creates convergent sequence to 1/2 scaling
%if index==5, creates convergent random sequence to 1/2 scaling

if ind==0
%usual sierp gasket
P=ones(3^(N+2)-3,1)./2;
end
```

```
if ind==1
%disconnected sierp dust of size 1/3
P=ones(3^(N+2)-3,1)./3;

end

if ind==2
%connected, random between two values
P=[];
for i=1:(3^(N+1)-3)/6
R=(rand(3,1).*(1/4))+(ones(3,1).*(3/8));
P=[P;R;ones(3,1)-R];
end
end
if ind==3
%want it to keep an ok amount, but not be connected and not too small
P=[];
for i=1:(3^(N+1)-3)/6
R=(2*rand(3,1)+3*ones(3,1))./8;
P=[P;R;6*ones(3,1)./7-R];
end
end

if ind==4
%convergent sequence to the usual 1/2 scaling
%       P=[1/4; 1/4; 1/4; 1/2; 1/4; 1/4];
```

```
P=[];

for i=1:(3^(N+1)-3)/6
R=[(1/2)+((-1)^i)/(8*i^(1/2)); (1/2)+((-1)^i)/(8*i^(1/2));
(1/2)+((-1)^i)/(-10*i^(1/2))];
P=[P;R;ones(3,1)-R];
end
end

if ind==5
%creates convergent random sequence to 1/2 scaling
P=[];

for i=1:(3^(N+1)-3)/6
T=(2*rand(1)-1)/3;
U=(2*rand(1)-1)/3;
V=(2*rand(1)-1)/3;
R=[(1/2)+T/(i^(1/2)); (1/2)+U/(i^(1/2));(1/2)+V/i];
P=[P;R;ones(3,1)-R];
end
end

if ind==6
%1-variable vvariable case
P=ones(3^(N+2)-3,1)./3;
P(1)=1/2;
P(2)=1/2;
```

```
P(3)=1/2;
P(4)=1/2;
P(5)=1/2;
P(6)=1/2;

end
end
```

```
function [M] = nextgen(L,k,P)
%k is the generation of L
%L is kth generation
%P is (6*3^k)x1 vector of proportions for new generation
%M is (k+1) generation

M=[];
if k==0
[T,R,S]=triangle(L,P);
M=[T;R;S];
else
for i=1:3^k
[T,R,S]=triangle(L(2*i-1:2*i,:),P(6*(i-1)+1:6*i));
M=[M;T;R;S];
end
end

end
```

```
function [T,R,S]=triangle(X,P)
%X is a 2*3 matrix of triangle vertices;
%P is a 6*1 matrix of new proportions
% T,R,S are three 2*3 matrix of new triangle vertices;
A=X(:,1); B=X(:,2); C=X(:,3);
T=[A,(1-P(1))*A+P(1)*B,(1-P(2))*A+P(2)*C];
R=[(1-P(4))*B+P(4)*A,B,(1-P(3))*B+P(3)*C];
S=[(1-P(5))*C+P(5)*A,(1-P(6))*C+P(6)*B,C];

end
```

```
function P= onevariable(N,ind)

%Input number of generations N

P=[];
if ind==0
%usual sierp gasket, one IFS
P=ones(3^(N+2)-3,1)./2;
end

IFS1=ones(3,1)./2;
IFS2=ones(3,1)./3;
if ind==1
%usual sierp gasket, 2 IFS to choose from

for i=1:N
```

```
r=rand(1);
for j=((3^(i)-3)/2)+1:(3^(i+1)-3)/2

if r>1/2
S=IFS1;
R=[S;ones(3,1)-S];
else
S=IFS2;
R=[S;S];
end

P=[P;R];

end
end
end
end
```

A.3. Menger Sponge functions

```
function S = modsponge(X,N,ind)
%X is initial cube/parallelogram 3x4 matrix
%N is generation

%SEE generateP FOR INDEX MEANINGS

%P is 6*20^kx1 sequence of proportions with P_2i <P_2i+1

if isempty(X)
```

```
X=[0 1 0 0;0 0 1 0; 0 0 0 1];
end
P=generateP(N,ind);

S=X;
M=X;
for k=1:N
M=newgen(S,k-1,P(((20^(k-1)-1)/19)*6+1:((20^k-1)/19)*6));
S=M;
end


figure
for i=1:length(M(:,1))/3
% for i=2:2
newO=M([3*i-2:3*i],1);
newA=M([3*i-2:3*i],2);
newB=M([3*i-2:3*i],3);
newC=M([3*i-2:3*i],4);
H=[newO newA newB newC (newA+newB-newO) (newA+newC-newO)
(newB+newC-newO) (newA+newB+newC-2*newO)]';
fill3(H([1 2 5 3],1), H([1 2 5 3],2),H([1 2 5 3],3),'c');
hold on
fill3(H([1 2 6 4],1), H([1 2 6 4],2),H([1 2 6 4],3),'b');
fill3(H([1 3 7 4],1), H([1 3 7 4],2),H([1 3 7 4],3),'g');
fill3(H([2 5 8 6],1), H([2 5 8 6],2),H([2 5 8 6],3),'y');
fill3(H([4 6 8 7],1), H([4 6 8 7],2),H([4 6 8 7],3),'m');
```

```
fill3(H([3 5 8 7],1), H([3 5 8 7],2),H([3 5 8 7],3),'r');
end
axis([0 1 0 1 0 1])
axis off


end
```

```
function [P] = generateP(N,ind)
%N is number of iterations wanted
%ind==0 gives usual menger sponge
%ind==1 gives random menger sponge
%ind==2 gives sequence converging to usual 1/3 scale, across iterations
%ind==3 gives convergent sequence converging to 1/3, but
across generations

if ind==0
P=ones(6*20^N,1);
for i=1:6*20^N
P(2*i-1)=1/3;
P(2*i)=2/3;
end
end

% if ind==1%if index==4, creates convergent sequence to 1/2 scaling
%       P=ones(6*20^N,1);
%       for i=1:(6*20^N)/2
```

```
%       R=rand(1,1)/2;
%       P(2*i-1)=R;
%       P(2*i)=1-P(2*i-1);
%       end
% end

if ind==1
%random between 0.32 and 0.35
P=ones(6*20^N,1);
for i=1:(6*20^N)/2
R=(3*rand(1,1)/100)+0.32;
P(2*i-1)=R;
P(2*i)=1-P(2*i-1);
end
end

if ind==2
%sequence converging to usual 1/3 scale, across iterations
P=ones(6*20^N,1);
for i=1:20^N
P(6*i-5)=(1/3)+((-1)^i)/(12*(i+1)^2);
P(6*i-3)=(1/3)-((-1)^i)/(6*(i+1)^2);
P(6*i-1)=(1/3)+((-1)^i)/(18*(i+1)^2);
P(6*i-4)=1-P(6*i-5);
P(6*i-2)=1-P(6*i-3);
P(6*i)=1-P(6*i-1);
end
```

```
end

if ind==3
%convergent sequence converging to 1/3, but across generations
P=[];
A=zeros(6,1);
for i=1:N
A(1,1)=A(1,1)+(1/3)+1/(12*i);
A(2,1)=A(2,1)+ (2/3)-(1/(12*i));
A(3,1)=A(3,1)+ (1/3)-(1/(12*(i^2)));
A(4,1)=A(4,1)+ (2/3)+(1/(12*(i^2)));
A(5,1)=A(5,1)+ (1/3)+(1/(12*(i^3)));
A(6,1)=A(6,1)+ (2/3)-(1/(12*(i^3)));

for k=1:6*20^(i+1)
P=[P;A];
end
end
end

end
```

```
function [M] = newgen(L,k,P)
%k is the generation of L
%L is kth generation
%P is (6*20^k)x1 vector of proportions for new generation
%M is (k+1) generation
```

```
M=[];
 if k==0
M=cube(L,P);
 else
 for i=1:20^k
N=cube(L(3*(i-1)+1:3*i,:),P(6*(i-1)+1:6*i));
M=[M;N];
 end
 end


 end
```

Bibliography

[1] Assouad, P. *Ètude d'une dimension mètrique lièe à la possibilitè de plongements dans* $\mathbb{R}^n$. Comptes Rendus de l'Acadèmie des Sciences, Sèrie A-B. 288 (15): A731–A734. (1979)

[2] Barnsley, M.F., *Fractals Everywhere*, Academic Press Professional, Inc. San Diego, CA, USA (1988)

[3] Barnsley, M.F., Vince, A., *Developments in fractal geometry*, Bull. Math. Sci, 3:299-348 (2013)

[4] Barnsley, M.F., Hutchinson, J.E., Stenflo, O., *V-variable fractals: fractals with partial similarity.* Adv. Math. 218, 2051–2088 (2008)

[5] Barnsley, M.F., Hutchinson, J.E., Stenflo, O., *V-variable fractals: dimension results.* Forum Math. 24, 445–470 (2012)

[6] Barnsley, M.F., Vince, A., *Developments in fractal geometry.* Bull. Math. Sci. 3, 299-348 (2013)

[7] Beardon, A. *On the Hausdorff dimension of general Cantor sets.* Mathematical Proceedings of the Cambridge Philosophical Society, 61(3), 679-694 (1965)

[8] Bedford, T., *Applications of dynamical systems to fractal—A study of cookie-cutter Cantor sets.* Fractal Geometry and Analysis (eds. Bélaire, J., Dubuc, S.), Canada: Kluwer, 1–44 (1991)

[9] Ben-Artzi, A., Eden, A., Foias, C., Nicolaenko, B. *Hölder continuity for the inverse of Mañè's projection*, Journal of Mathematical Analysis and Applications, 178 (1), 22-29 (1993)

[10] Climenhaga, V., Pesin, Y., *Lectures on Fractal Geometry and Dynamical Systems*, AMS Student Math. Lib. V. 52, (2009)

[11] Falconer, K. *Random fractals.* Math. Proc. Cambridge Philos. Soc. 100 (3), 559-582, (1986)

[12] Falconer, K. *Fractal Geometry: Mathematical Foundations and Applications*, Wiley, ISBN: 9780470871355 (2014)

[13] Fernández-Martínez, M., Sánchez-Granero, M. *Irreducible fractal structures for Moran type theorems.* Chaos, Solitons and Fractals. 119 (2017)

[14] Fraser, J. *Assouad type dimensions and homogeneity of fractals*, Transactions in the AMS, 366(12), (2013)

[15] Gulick, D., *Encounters with Chaos and Fractals*, Chapman & Hall/CRC, (2012)

[16] Hausdorff, F. *Dimension und ausseres mass*, Math. Ann. 79, 157-179 (1919)

[17] Holland, M. and Zhang, Y., *Dimension results for inhomogeneous Moran set constructions.* Dyn. Syst., 28(2):222–250, (2013)

[18] Hua, S., Rao, H., Wen, Z. et al. *On the structures and dimensions of Moran Sets*, Sci. China Ser. A-Math. 43: 836 (2000)

[19] Hutchinson, J., *Fractals and Self-Similarity* Indiana University Math. J. 30 (5), 713-747 (1981)

[20] Jia, B. *Bounds of Hausdorff measure of the Sierpinski gasket*, J. Math. Anal. Appl, 330, 1016-1024, (2007)

[21] Li, J. *Assouad dimensions of Moran sets.* C.R. Acad. Sci. Paris, Ser. I, 351, 19-22 (2013)

[22] Li, W., Li, W., Miao, J., Xi, L. *Assouad dimensions of Moran sets and Cantor-like sets* Frontiers of Matematics in China, 11 (3), 705-722 (2016)

[23] Li, W., Xiao, D., *A note on generalized Moran set.* Acta Math. Sci. (Suppl.) 18 88-93 (1998)

[24] Ma, J., Rao, H., Wen, Z., *Dimensions of cookie-cutter-like sets* Science in China, Series A: Mathematics, 44, 1400-1412 (2001)

[25] Mandelbrot, B. B. *The fractal geometry of nature.* San Francisco, California: W. H. Freeman and Co. (1982)

[26] Mauldin, R. D., Urbanski, M., *Dimensions and Measures in Infinite Iterated Function Systems*, Proc. London Math. Soc., 73(3):105 (1996)

[27] Mauldin, R. D., Williams, S. C., *Hausdorff Dimension in Graph Directed Constructions* Trans. of the AMS, 309 (2), (1988)

[28] McMullen, Curt. *The Hausdorff dimension of general Sierpiński carpets.* Nagoya Math. J. 96, 1–9. (1984)

[29] Moran P.A.P. *Additive functions of intervals and Hausdorff measure.* Proc. Camb. Philos. Soc, **42**, 15-23 (1946)

[30] Peres, Y., Rams, M., Simon, K., Solomyak, B. *Equivalence of Positive Hausdorff Measure and the Open Set Condition for Self-Conformal Sets*, Proc. of the AMS, 129 (9), 2689-2699 (2001)

[31] Peres, Y., Solomyak B. *Problems on self-similar sets and self-affine sets: An update*, Fractal Geometry and Stochastics II, Progress in Probability, 46, 95-106, (2000)

[32] Pesin, Y., Weiss, H., *On the Dimension of Deterministic and Random Cantor-like Sets, Symbolic Dynamics, and the Eckmann-Ruelle Conjecture.* Comm. Math. Phys., 182: 105. (1996)

[33] Pontryagin, L.S., Shnirel'man, L.G. *On a Metric Property of Dimension.* Annals of Math, 33, 156-162. (1932)

[34] Rajala, T., Vilppolainen, M., *Weakly controlled Moran constructions and iterated functions systems in metric spaces*, Illinois Journal of Mathematics, 55 (3), 1015-1051 (2011)

[35] Sánchez-Granero, M.A., Fernández-Martínez,M. *Irreducible fractal structures for Moran type theorems*, Chaos, Solitons and Fractals, 119, 29-36 (2019)

[36] Shief, A. *Separation properties for self-similar sets*, Proc. of the AMS, 122 (1), 111-115 (1994)

[37] Urbanski, M. *Parabolic Cantor sets* Fund. Math., 151 (3), 241-277 (1996)

[38] Wen, Z. *Moran sets and Moran Classes.* Chinese Science bulletin, 46 (22), 1849-1856 (2001)

[39] Zhou, Z. *Hausdorff measure of Sierpinski gasket*, Science in China (Series A), 40 (10), (1997)